Università degli Studi di Ferrara

DOTTORATO DI RICERCA IN
BIOCHIMICA, BIOLOGIA MOLECOLARE E BIOTECNOLOGIE

CICLO XXII

COORDINATORE Prof. FRANCESCO BERNARDI

VIRUSES & PARASITES:
surface mapping of Env glycoprotein from HIV and role of hexose-6-phosphate mutarotase from *Trypanosoma brucei* in oxidative stress

Settore Scientifico Disciplinare BIO/10

Dottorando
Dott. Magnani Morena

Tutore
Dott. Hanau Stefania

Anni 2007/2009

INDEX

PART I: surface mapping of Env glycoprotein from HIV **5**

INTRODUCTION **6**

HIV and AIDS 6

The physical and genetic structure of HIV 8

The life cycle of HIV 9

Immune response to HIV 11

Cellular immune responses 13

Immune system failure to contain HIV 15

Tat protein 16

Env protein 17

Tat-Env 20

HIV protein-based vaccine 20

AIM OF THE THESIS **22**

MATERIALS AND METHODS **23**

gp120 and gp140 23

Counting the number of modified lysine residues of gp140 and gp120 envelope proteins 23

Fluorometric detection of cysteine derivatives of gp120 and gp140 envelope proteins 24

HPLC 25

Mass spettroscopy 25

RESULTS AND DISCUSSION **26**

PART II: role of hexose-6-phosphate mutarotase from *Trypanosoma brucei* in oxidative stress **35**

INTRODUCTION **36**

Parasites 36

Human African Trypanosomiasis 37

The Trypanosoma brucei 39

Life cycle 41
Energy metabolism 42
Defence against oxidative stress in Trypanosomes 46
Anomeric specificity of enzymes 46
Hexose-6-phosphate mutarotase 48
State of the art on H6PM from T. brucei 49
AIM OF THE STUDY **52**
MATERIALS AND METHODS **53**
Overexpression of the T. brucei enzyme in E. coli. 53
Purification of recombinant protein 53
Determination of protein concentration 54
Electrophoresis in polyacrylamide gel (SDS PAGE) 54
Storage of the enzyme 54
Kinetic studies 54
Preparation of α-glucose 55
G6PDH-Assay 55
RNA interference 56
RNAi construct 57
Linearization of plasmid 58
Spectrophotometric determination of DNA concentration 58
Electrophoresis in agarose gel 59
Transfection of trypanosomes and growth curve 59
Bloodstream form transfection 59
Procyclic transfection 60
RT-PCR 60
Hydroperoxide-sensitivity assay 62
RESULTS **63**
Conditional depletion of H6PM levels by RNAi 63
Growth curves 63

RT-PCR 65
Sensitivity of H6PM-RNAi bloodstream cell lines toward oxidative stress 66
Protein purification from *E.coli* 70
Activity assay 71
Stability of recombinant *T.brucei* H6PM 73
DISCUSSION **74**
REFERENCES PART I **76**
REFERENCES PART II **80**

PART I:
surface mapping of Env glycoprotein from HIV

INTRODUCTION

HIV and AIDS

The Human Immunodeficiency Virus (HIV) is a retrovirus of the lentivirus family. Lenti means slow, and the name reflects the long incubation period, the time it takes from infection until the associated disease starts developing. The virus is mainly transmittable through bodily fluids, primarily blood and semen. A person infected with the virus has a gradual inactivation of the immune system. Characteristically, the CD4+ T cells are depleted. This causes the disease Acquired Immunodeficiency Syndrome (AIDS). With their immune system in disarray the bearer of the virus is more susceptible to opportunistic infections and several, otherwise rare, types of cancer.

AIDS is now a pandemic disease. In 2007, it was estimated that 33.2 million people lived with the disease worldwide, and that AIDS killed an estimated 2.1 million people, including 330.000 children. Over three-quarters of these deaths occurred in sub-Saharan Africa.

Several steps are being taken to combat this disease. One important step is health education campaigns that inform the public of how AIDS is transmitted, thereby trying to limit the number of people being exposed to the virus. Another step is the development of drugs to treat the disease. Research that gives us knowledge of the molecular mechanisms of how the virus interacts with its host will drive forward the development of novel therapies. No known therapy can completely rid the body of the virus. Several vaccines are currently in different stages of clinical trials in humans. These vaccines are, however, therapeutic vaccines, aimed at controlling the infection rather than preventing it (reviewed by Amara and Robinson, 2002). A combination of drugs called HAART (Highly Active Anti-Retroviral Therapy) has proved very efficient in stalling the disease, but there are serious problems with toxic side effects (Louie *et al.,* 2002; http://hivmedicine.com/index.htm).

A major problem in the development of treatments and therapies for HIV infection is the high frequency with which the virus mutates. Mutations also cause the changes that make the immune system unable to recognize the virus (Wei *et al*., 2003). The viral encoded reverse transcriptase protein (RT) transcribes genomic RNA to double stranded DNA, which is integrated into the host genome. RT does not have a proof-reading activity, and is the main cause of mutations of the virus (Preston and Dougherty, 1996). This accounts for the many different strains and subtypes of HIV.

HIV is classified as two major types: HIV-1 and HIV-2. HIV-1 is the most common and infectious of these two, and can further be divided into 3 groups: M, N and O. HIV-1 Group M is by far the most important contributor to the AIDS pandemic and can further be divided into 10 subtypes, A-H and J-K (http://hiv-web.lanl.gov). When comparing the sequences of different strains of HIV with those of Simian Immunodeficiency Virus (SIV), the interspersion in the evolutionary tree (see

figure 1) suggests shared viral lineages (Hahn *et al.*, 2000; Korber *et al.*, 2000), and that HIV has arisen when SIV has been transmitted from its natural simian host to humans. It also suggests that this sort of transmission has occurred several times. For instance, it is likely that HIV-1 groups M, N and O have arisen from separate zoonotic transmissions of SIV. HIV-1 and HIV-2 are related to quite different strains of SIV, SIV from chimpanzees, SIVCPZ, and sooty mangabey, SIVSM, respectively. Despite its name, most strains of SIV do not cause disease in their natural host.

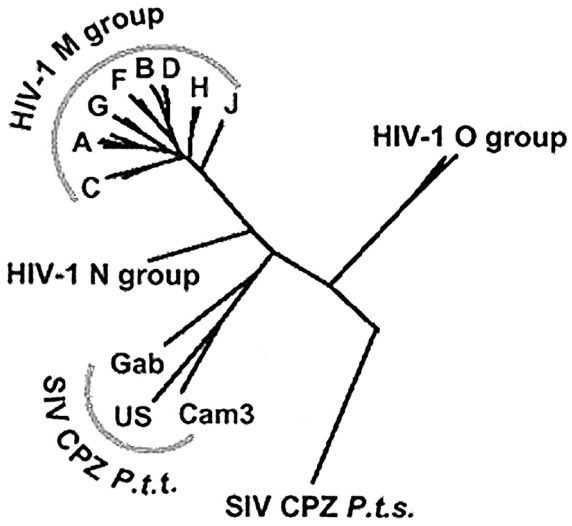

Figure 1: Phylogenetic (i.e. evolutionary) tree of different strains of HIV-1 and SIV CPZ, showing how they are related. The length from one indicated point to another shows relative genetic distance. HIV-1 group M is the main cause of the global pandemic and all the subtypes within are likely to have descended after a single zoonotic transfer (cross-species transfer from the natural host, a non-human, to a human) of a simian virus. HIV groups N and O are likely to have arisen after separate zoonotic transmissions. SIV CPZ P.t.t.: strains of SIV found in *Pan troglodytes troglodytes*, a subspecies of chimpanzee. SIV CPZ P.t.s.: a strain of SIV found in a chimpanzee of the subspecies *Pan troglodytes schweinfurthii*. (Modified from Reeves and Doms, 2002)

A sample from 1959 shows that HIV-1 was in a human population already at that time (Zhu *et al.* 1998) and sequence analyses estimate that the last common ancestor of the HIV-1 M group existed in a human host some time between 1915 and 1941 (Korber *et al.* 2000).

What effect the divergence in sequence between the different strains has on virulence, transmission rates and general epidemiology has not been clarified, but the different HIV-1 types all have the same basic structure (shown in figure 2), and the same life cycle (figure 4).

The physical and genetic structure of HIV

A model of the virus particle is depicted in figure 2. It is spherical with a membrane that originates from the host cell plasma membrane. Located on the surface of the membrane is a protein called gp120 or the Surface protein (SU). It is anchored through gp41, the Transmembrane protein (TM). TM is embedded in the membrane. Underneath the plasma membrane is an icosahedron made by the Matrix protein (MA). Inside the icosahedron the Capsid protein (CA) forms a cone in the mature virus particle. This cone is called the core particle. Within this cone are the proteins Reverse Transcriptase (RT), Integrase (IN), Protease (PR), and Nucleocapsid (NC). The latter is associated with the two RNA copies of the HIV genome. This association serves to stabilize the genome. In addition the viral particle contains the viral proteins Nef, Vif, Vpr and p6, as well as several cellular factors (Frankel and Young 1998; Ott *et al.*, 2000). Among these is the tRNA (tRNALys) that is used as primer for initiation of reverse transcription.

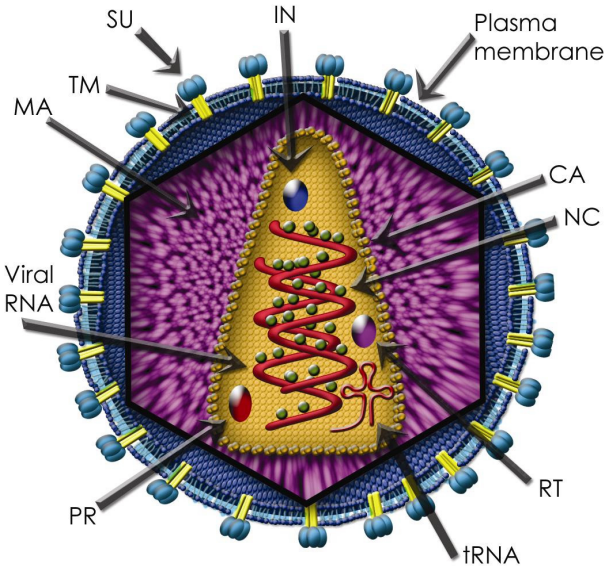

Figure 2: Organisation of the HIV-1 virus particle, showing the most important parts

Depicted in figure 3 is the organisation of the HIV-1 genome, an approximately 9200 bp long single stranded RNA. It contains the *gag*, *pol* and *env* genes. This is typical for all retroviruses. These genes encode polyproteins, which are cleaved by proteolysis into individual proteins. The Gag polyprotein is cleaved into the proteins MA, CA and NC that make up the core of the virion, as well as p6 found within the virion. *Env* encodes the membrane proteins SU and TM. *Pol* encodes the enzymes PR, RT and IN. The HIV genome further contains the genes for Tat and Rev, proteins that

regulate HIV gene expression, as well as genes for four accessory proteins, Nef, Vif, Vpr and Vpu. As seen in the figure, these additional proteins are encoded by separate and overlapping ORFs (Frankel and Young, 1998).

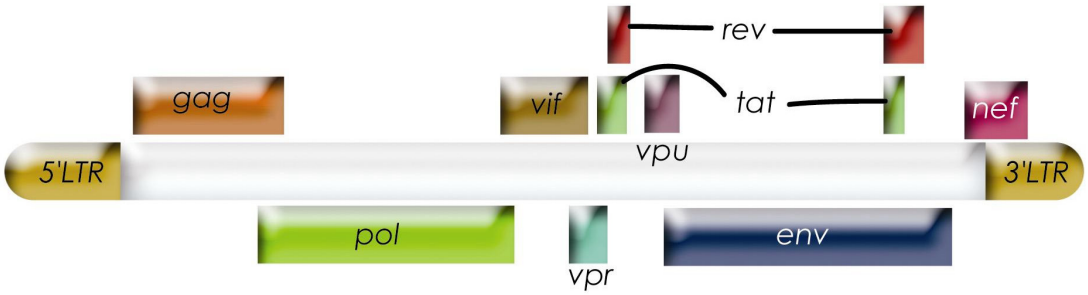

Figure 3: The HIV-1genome. The genes *gag*, *pol* and *env* encode polyproteins that are proteolytically cleaved to produce the mature virion proteins. The viral protease (PR) cleaves Gag and Gag-Polpolyproteins, while the Env polyprotein is cleaved by a cellular protease. *Gag* encodes the Matrix protein (MA), the major Capsid protein(CA), the Nucleocapsid protein (NC) and p6; from *pol*, Protease, Reverse Transcriptase (RT) and Integrase (IN); and from *env*, the surface subunit (SU) gp120 and the Transmembrane subunit (TM) gp41 are encoded. The regulatory proteins Tat and Rev, as well as the accessory proteins Vif, Vpr, Vpu and Nef are all encoded by their own open reading frames in the HIV-1genome. The Long Terminal Repeat, LTR, is used as a promoter. The HIV-1 mRNA contains several splicing sites. Fully spliced it encodes Tat, Rev and Nef proteins. The other proteins are expressed when Rev downregulates the splicing of this mRNA. The proteins encoded by *gag* and *pol* also have alternate names, based on their molecular weight. MA=p17, CA=p24, NC=p7,RT=p66/p51 (a dimer where the two subunits are differently cleaved), IN=p32, PR=p11.

The life cycle of HIV

The life cycle of HIV is outlined in figure 4. HIV-1 infects a cell as the plasma membrane of the virus particle fuses with the cellular plasma membrane. This is a result of the interaction between SU in the viral membrane and the cell-surface receptor CD4. The fusion of these membranes also requires a coreceptor. The coreceptor commonly used by HIV-1 is CXCR4, which is located on the surface of CD4 T Helper cells; or CCR5, which is located on the surface of macrophages and a subset of the CD4 T Helper cells (figure 5). Which coreceptor a virus can use determines its tropism. The fusion of viral and cellular membranes leads to the release of the viral core particle into the cytoplasm. The particle develops into a looser structure. Within this structure the RNA genome is reverse transcribed. This renders a linear double stranded DNA molecule. The transformed core particle, a DNA protein complex called the preintegration complex (PIC), moves from the cytoplasm into the nucleus. There IN integrates the viral DNA into a host chromosome, thus making the viral genome a stable genetic element of the infected cell, a provirus.

The first full-length viral mRNAs to be produced will for the most part be doubly spliced. These mRNAs encode the Tat, Rev and Nef proteins. Tat and Rev function in feedback loops and will travel to the nucleus. Tat will increase the production of functional HIV mRNAs through a mechanism discussed later. Rev transports unspliced and singly spliced viral mRNAs to the cytoplasm where the mRNAs are translated. This leads to the expression of the other HIV proteins.

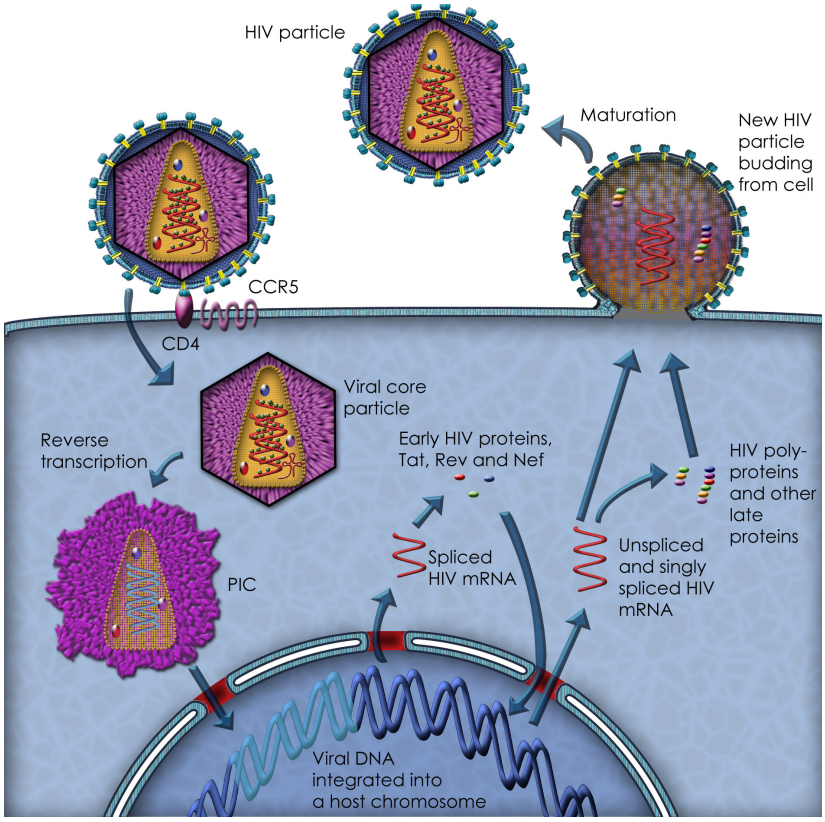

Figure 4: The HIV life cycle

Full-length, unspliced mRNA transcribed from the provirus is packaged into the new virions and used as genomic RNA. It is also used as messenger RNA for synthesis of both Gag and Gag-Pol polyproteins. The latter is made when the ribosome shifts reading frames while translating this mRNA. This happens approximately every 20th round of translation. The Gag and Gag-Pol polyproteins will associate at the plasma membrane and initiate the assembly of the core particle. The plasma membrane where they assemble is enriched with the SU and TM proteins. These two proteins are formed as gp160 polyprotein and cleaved by a cellular protease in the Golgi. The core particle becomes encapsulated within plasma membrane as it is budded off from the cell. Maturation takes place during or immediately after the budding of this particle. A functional core

particle is formed in this process when the viral protease cleaves the Gag and Gag-Pol polyproteins (reviewed by Frankel and Young, 1998).

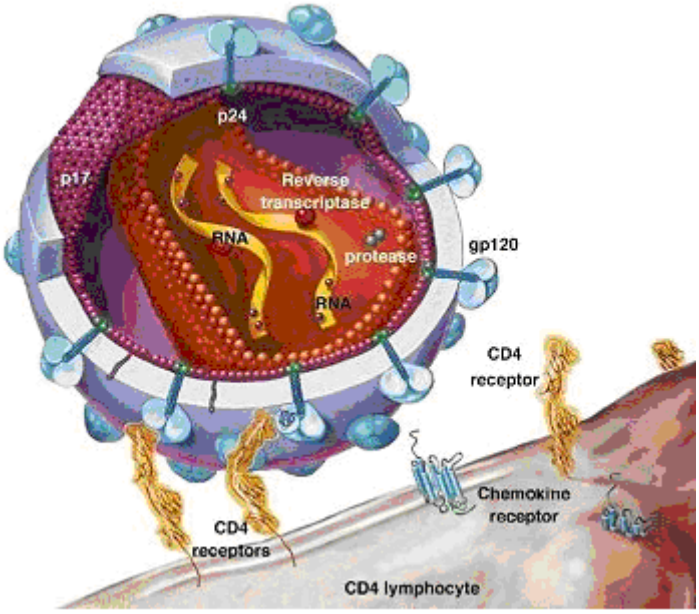

Figure 5: HIV binding via cell surface receptor

Immune response to HIV

Exposure to a pathogen elicits innate or adaptive (acquired) immune responses. Innate responses are immediate and nonspecific, and do not result in immunological memory but limit damage before adaptive immune responses take effect. The latter develop over days to weeks after exposure to antigen, through clonal expansion and differentiation of B lymphocytes and T lymphocytes, which recognize antigen via specific binding of cell surface receptors. A proportion of antigen-specific lymphocytes differentiates into memory cells; these characteristically respond more rapidly following re-exposure to the stimulating antigen (a phenomenon exploited by active immunization). Adaptive immune responses to HIV are detectable in all infected individuals at some time and comprise antibodies and CD8+ (cytolytic) and CD4+ (helper) T cells.

Following acute infection, HIV disseminates throughout the lymphoid system and replicates in a subset of CD4+ T cells, generating up to 10^{10} new virus particles per day. Within 2–3 weeks, the concentration of virions in the circulation (expressed as the number of copies of viral genomic RNA/ml plasma) reaches a peak of several million; this declines over the following months to a ‘set-point’ or steady-state level. The set-point is predictive of the rate at which individuals progress to AIDS. The virus population at this point is not genetically homogeneous, but is a mixture of a

large number of genetically mutated strains, present because of a lack of 'proof-reading' by reverse transcriptase (the enzyme that makes DNA copies of viral genomic RNA). Although early immune responses determine the level of the viral load set-point, the high mutation rate of HIV is an important factor in the ultimate failure of the immune system to contain it.

Antibodies specific responses to a range of HIV proteins typically develop over 4–6 weeks after infection, and their detection by enzyme-linked immunosorbent assay (ELISA) is the basis of the most widely used diagnostic test for HIV infection. During acute infection, the concentration of antibodies in the circulation may be too low to be detected by ELISA, and serological tests performed during this 'window period' may give a false-negative result.

Although antibody binding of cell-free virus in the circulation and at mucosal surfaces contributes to the clearance of many viral infections, and pathogen-specific antibodies are typically a marker of protective immunity, this is not usually the case in HIV infection. Antibodies to structural proteins (Gag, p24 and p17) appear first, are non-neutralizing and do not generally persist. Antibodies with neutralizing capacity appear later and are detectable throughout the course of infection. They are predominantly targeted at one of three regions in the envelope protein that are crucial for viral entry into CD4+ T cells (Figure 6):

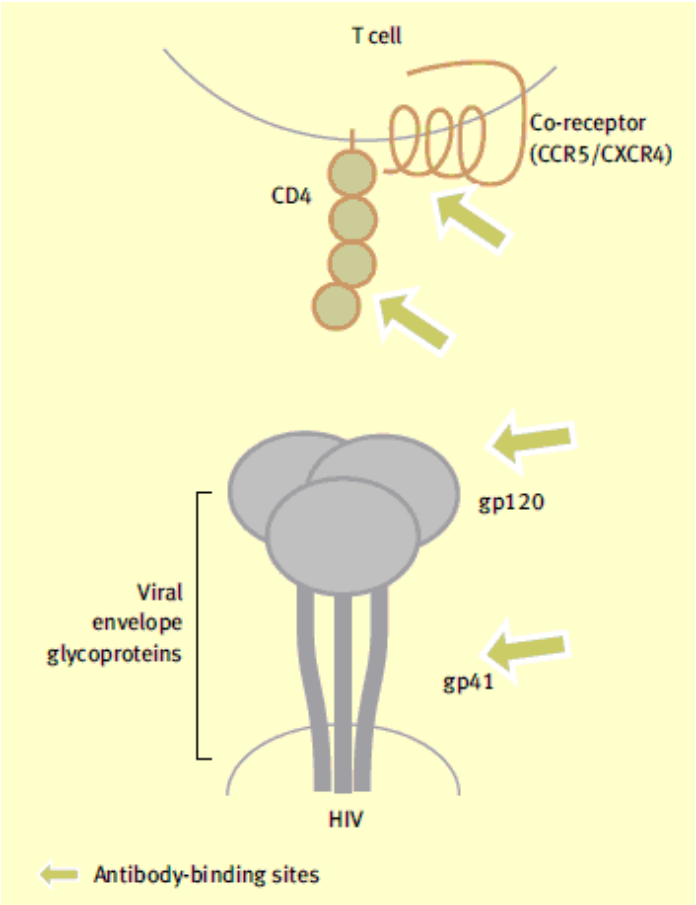

Figure 6: Targets of the antibody response in HIV infection

• a variable region (V3 loop) of a subunit protein, gp120
• the binding sites for CD4 and the chemokine receptors CXCR4 and CCR5
• the transmembrane protein gp41.

However, antibodies in the sera of HIV-infected individuals are principally directed at irrelevant regions of the envelope protein or at virion debris, and have weak neutralizing capacity.

Over time, mutant viruses emerge that can evade a previously effective neutralizing response. Although this is indicative of immune selective pressure, there is no conclusive evidence that escape from neutralizing antibody responses is associated with disease progression; thus, they appear to contribute little to the control of HIV replication once infection is established. Certain individuals who remain symptom-free and maintain a low viral load and stable CD4 T cell count for up to 20 years (long-term non-progressors, LTNPs) have a strong neutralizing antibody response, but this is not a universal finding in this group of patients.

Cellular immune responses

HIV-specific cellular immune responses are triggered after virus entry into target cells and subsequent synthesis of viral proteins. HLA (MHC) class I molecules on the cell surface display peptide fragments of degraded intracellularly derived viral proteins for recognition by specific T cell receptors (TCRs) on CD8+ T lymphocytes. CD4+ T lymphocyte TCRs recognize HLA class II-bound peptides generated by the processing of shed viral proteins in specialized antigen-presenting cells, dendritic cells and macrophages. Engagement of the TCR with HLA–peptide complexes activates T cell effector functions. Generally, cytolytic CD8+ T cells lyse HIV-infected cells and secrete soluble factors, cytokines (interferon-γ (IFN-γ), tumour necrosis factor α) and chemokines (MIP-1α, MIP-1β and RANTES) that suppress virus replication or block viral entry into CD4+ T cells; CD4+ or T helper cells secrete cytokines that modulate the functions of other cell types (Figure 7).

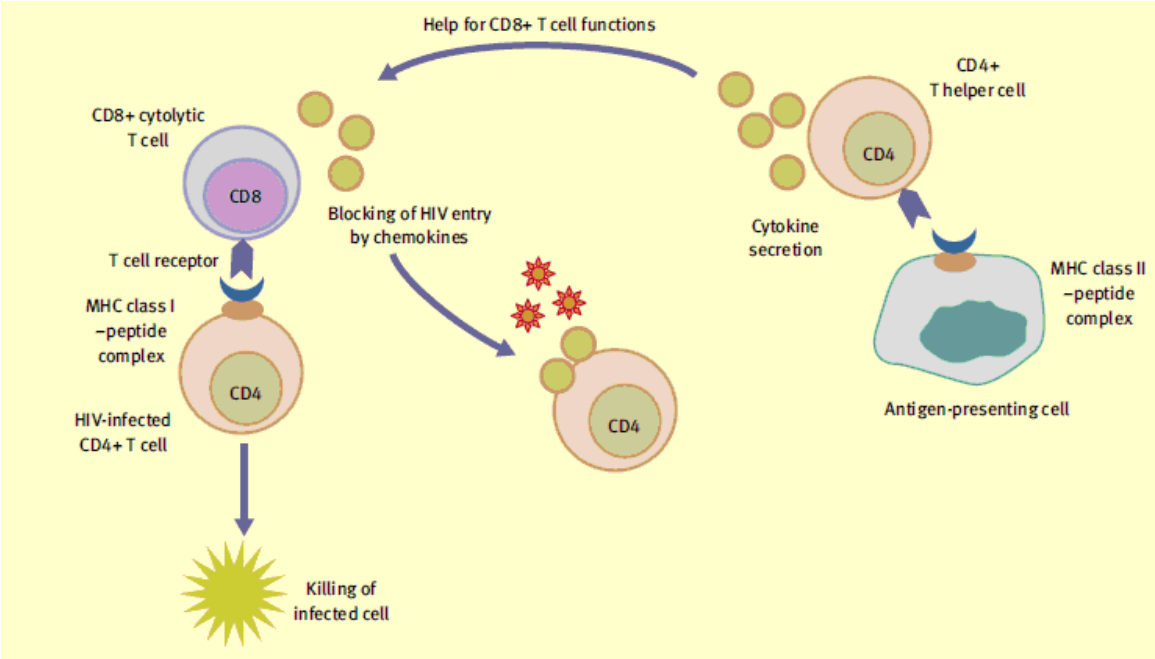

Figure 7: Function of virus-specific T cells

Most HIV-infected individuals develop vigorous, virus-specific CD8+ T cell responses that may be detectable within weeks of infection, before seroconversion. Evidence suggests that they are crucial for control of HIV replication in vivo. The appearance of cytolytic CD8+ T cells coincides with the decline in viraemia after primary infection. Virus variants that escape CD8+ T cell recognition emerge over time, indicating that selective pressure exerted by CD8+ T cell responses shapes the evolution of the virus population in infected individuals. Heterozygosity for HLA class I alleles, which determine selection of viral peptides for presentation to CD8+ T cells, or the presence of certain alleles (HLA B27 or B57), is associated with a lower set-point viral load and slower disease progression. Treatment of simian immunodeficiency virus (SIV)-infected macaques with a monoclonal antibody to deplete CD8+ T cells results in a marked increase in SIV viraemia that is suppressed when CD8+ T cells are restored.

CD4+ T cells are conventionally detected by in vitro T cell proliferation assays. Because CD4+ T cell proliferative capacity is lost early in infection in most HIV-infected individuals, it was assumed that these cells contribute little to the control of HIV replication. However, sensitive assays detecting cytokine release indicate that HIV-specific CD4+ T cells are present during chronic infection, and recent research suggests that the type and range of cytokine secretion may correlate with viraemia control. The presence of CD4+ T cells secreting the growth factor interleukin-2 (IL-2), or cytokines including IL-2 and IFN-γ, is more favourable than that of cells secreting IFN-γ alone. Strong HIV-specific CD4+ T cell proliferative responses, in tandem with vigorous CD8+ T

cell responses, have been seen in LTNPs and this, together with the role of CD4+ T cells in facilitating and maintaining both antibody and CD8+ T cell effector and memory responses in other viral infections, suggests that effective CD4+ T cell help is important for containment of HIV.

Immune system failure to contain HIV

Less than 2% of infected individuals can be reliably defined as LTNPs; most of them present progressive CD4+ T cell depletion and develop symptoms related to immunodeficiency after a median of 10 years, despite evident HIV-specific immune responses. There are many reasons why the immune system fails to contain HIV replication. By establishing latent infection in long-lived CD4+ T cells, HIV can remain invisible to CD8+ T cells; therefore, infected cells are not destroyed. Virus replication can be initiated in these cells at a later stage, generating new infectious virions.

Specific properties of the virus envelope protein account for the resistance of HIV to antibody neutralization; extensive glycosylation and shielding of crucial antibody epitopes by non-immunogenic carbohydrate molecules prevents antibody blockade of the key sites in the envelope required for viral entry into CD4+ cells. Antibodies to the V3 loop (a major neutralizing determinant and one of the most antigenically variable regions of the envelope protein) are generally specific to a single HIV isolate and therefore exhibit poor neutralizing activity against other virus variants. The CD4-binding domain is highly conserved between virus strains, in contrast to the V3 loop, but antibodies specific to this region of the envelope exhibit weak neutralizing activity.

Antigenic variation within or close to CD8+ and CD4+ T cell epitopes can affect either the capacity of viral peptides to bind to MHC molecules, or the ability of TCRs to recognize the MHC–peptide complex. A single amino acid substitution may be sufficient to enable virus escape from T cell recognition, at any stage in the course of infection. The HIV Nef protein reduces expression of MHC class I molecules on the infected cell surface, thereby potentially impairing presentation of viral peptides to CD8+ T cells, though the contribution of this mechanism to immune failure is not known. HIV-specific CD8+ T cells may exhibit antiviral functions such as IFN-γ-secreting capacity, yet fail to proliferate in response to viral antigenic stimulation or exhibit impaired cytolytic capacity.

Functional impairment of CD4+ T cells is evident even before the absolute CD4+ T cell count has declined significantly. This may be attributable to preferential infection of HIV-specific CD4+ T cells and to replication of virus occurring predominantly in recently activated cells (i.e. those responding to the infection).

Tat protein

Tat *(trans-activator)* proteins are early RNA binding proteins regulating lentiviral transcription. These proteins are necessary components in the life cycle of all known lentiviruses, such as the human immunodeficiency viruses (HIV).

In acute infection of T cells by HIV, Tat is released extracellularly by infected cells [Ensoli et al. 1990; Westendorp et al. 1995] and is taken up by neighbour cells [Ensoli et al. 1993; Barillari et al. 1992]. Tat is also immunogenic and antibodies (Ab) against Tat have been found to correlate with delayed disease progression [Reiss et al. 1990; Zagury et al. 1998; Re et al. 1995] and may exert protective effects by inhibiting both HIV replication and the effects of extracellular Tat [Ensoli et al. 1993; Re et al. 1995]. Moreover, Tat is efficiently taken up by monocyte-derived dendritic cells (MDDCs), promotes their maturation and antigen (Ag)-presenting functions [Fanales- Belasio et al. 2002] directing Th1 and CTL responses against itself and other Ags since it enters the major histocompatibility complex (MHC) class I pathway [Kim et al. 1997]. Finally, vaccination of monkeys with a biologically active Tat protein or DNA has been shown to be safe, immunogenic and to contain infection with the highly pathogenic SHIV89.6P [Cafaro et al. 2000;Ensoli et al. 2000; Dominici et al.2003]

Tat proteins are thus ideal targets for drugs intervening with lentiviral growth. The consensus RNA binding motif (TAR, *trans-activation* responsive element) of HIV-1 is well characterized. Regarding Tat sequence in general, sequence regions corresponded to structural domains of the protein. The Tat protein contains 86 amino acids. It exhibits a hydrophobic core of 16 amino acids and a glutamine-rich domain of 17 amino acids. Part of the NH_2 terminus, Val4 to Pro14, is sandwiched between these domains. Two highly flexible domains correspond to a cysteine-rich and a basic sequence region. The 16 amino acid sequence of the core region is strictly conserved among the known Tat proteins (Bayer et al.1995)

```
         10         20         30         40         50         60         70
          |          |          |          |          |          |          |
MEPVDPRLEP WKHPGSQPKT ACTNCYCKKC CFHCQVCFIT KALGISYGRK KRRQRRRAHQ NSQTHQASLS
         80     86
          |      |
KQPTSQPRGD PTGPKE
```

Figure 8: Tat protein sequence(*Bioafrica)*

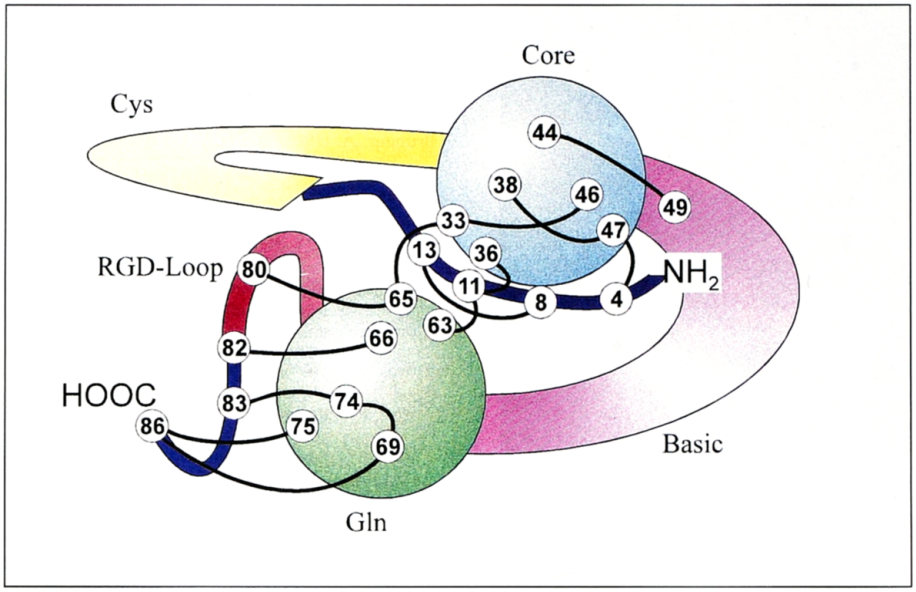

Figure 9: Tat protein domain

Env protein

The HIV envelope glycoproteins (Env) are organized on virions as trimeric spikes of noncovalently associated heterodimers of gp120 and gp41 that are assembled following cleavage of a gp160 precursor molecule.

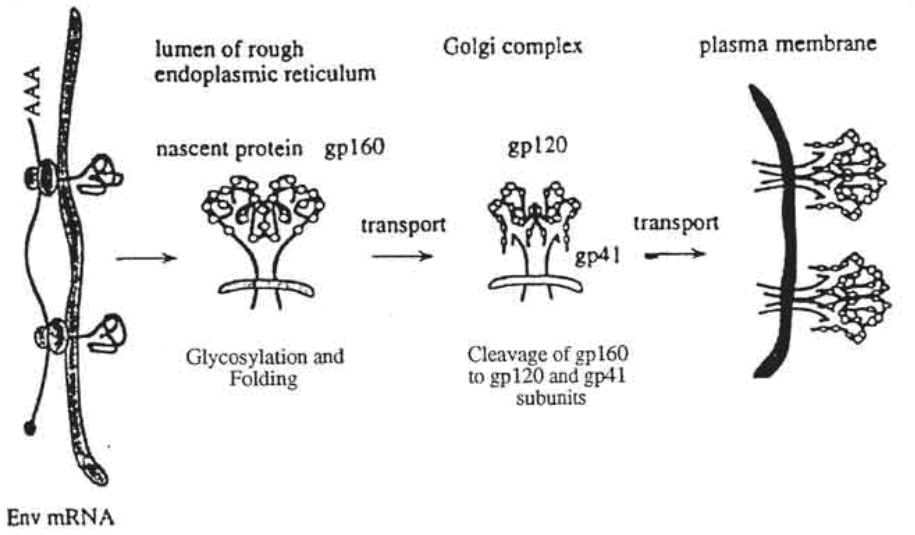

Figure 10: gp120-gp41 heterodimers assembling

The Env trimer mediates viral tropism and entry and is the target for neutralizing antibodies. Each virion contains approximately 5–10 spikes (Roux et al. 2007), although it has been estimated that

only one spike may be needed to mediate viral entry (Yang et al. 2005). Gp120 contains highly conserved binding sites for CD4 and a coreceptor, either CCR5 or CXCR4 (Pierson et al. 2003). Following engagement by CD4, gp120 undergoes extensive conformational changes that lead to coreceptor binding and release of gp41 to interact directly with the cell membrane. Thereafter, gp41 molecules undergo a cooperative structural rearrangement within the trimer that draws the viral and cell membranes together, initiating fusion and enabling viral entry.

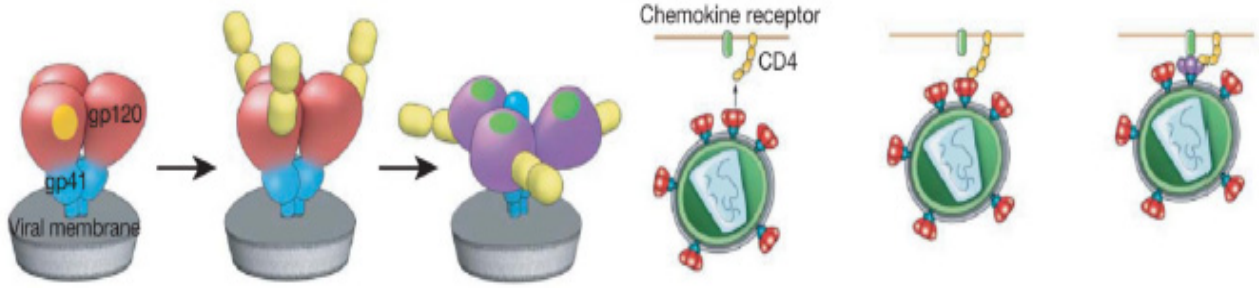

Figure 11: Conformational changes occuring upon CD4 binding.

All of these steps are critical for infection; thus, all are potential targets for antibody inhibition, but the Env has evolved an extensive array of defenses that either prevent neutralization or enable escape variants to emerge once neutralizing antibodies are made. Sites on gp120 for CD4 and coreceptor binding are located on a central core formed by an inner and outer domain that, in the context of an Env trimer, are surrounded by an extensive array of carbohydrates comprising up to 50% of gp120's molecular mass (Wyatt et al. 1998; Kwong et al. 1998; Kwong et al. 2009;). Because these carbohydrates are synthesized by host glycosylation machinery, they are largely nonimmunogenic and constitute an exposed but immunologically silent face (Wyatt et al. 1998). In addition, on a trimer, gp120 contains externally oriented variable loops (V1, V2, V3, and V4) that participate in poorly understood cooperative interactions to protect underlying core domains from antibody binding. Although these loops are highly immunogenic, they can tolerate extensive genetic diversity, and mutations within these sites, resulting from HIV's highly error-prone reverse transcriptase, enable the virus to escape neutralization (Frost et al. 2005). The V3 loop, which largely determines tropism for CCR5- or CXCR4-expressing CD4 cells and participates directly in coreceptor binding, was once viewed as the principal neutralizing determinant for antibodies (Hartley et al. 2005).

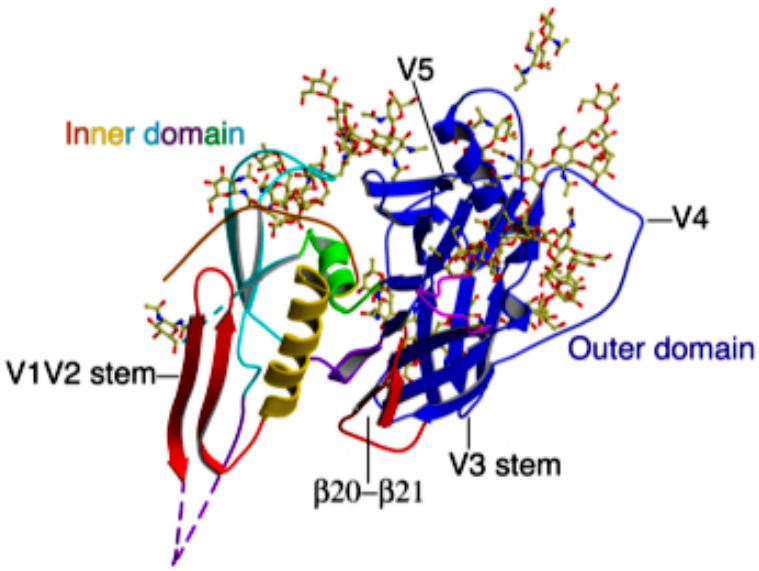

Figure 12: Env protein domains

However, it is now appreciated that in transmitted HIV isolates, this loop, although highly immunogenic, is largely concealed prior to CD4 attachment and binds poorly to antibodies (Binley et al.2004; Lusso et al. 2005; Li et al. 2005; Davis et al. 2009). Conformational defenses play additional roles. Prior to CD4 binding on the cell surface, the flexibility of gp120 may limit the formation of neutralization epitopes (Kwong et al. 2002); after CD4 binding, domains that are induced and that help to form a coreceptor binding site on the gp120 core are sterically restricted and inaccessible to antibodies (Labrijn et al. 2003). There are also Env surfaces that are not exposed on the trimer (i.e., the "non-neutralizing" face of gp120), which are highly immunogenic but elicit antibodies that cannot bind to an intact Env trimer (Wyatt et al. 1998). These domains, along with disrupted spikes on virions, are likely exposed in the context of gp120 shedding and viral debris from infected cells and may serve as immunodominant decoys to divert immune responses from potentially more efficacious but less immunogenic neutralization epitopes (Moore et al. 2006). Given the sparse distribution of Env trimers on a virion, antibodies also may be unable to bind with both of their Fab domains, further diminishing their potency (Klein et al. 2009). In general, it has become increasingly apparent that to neutralize HIV an antibody must bind to the Env trimer (27–29 Fouts et al. 1997; Kim et al. 2005; Sattentau et al 1995), and an understanding of potential binding sites on this structure is clearly needed.(Hoxie 2010)

Gp140 is a soluble protein with gp120 and gp41(containing the trimerization domain) fused together, it is the ectodomain of gp160, thus is an Env form stabilising the trimer.

A mutant of gp140 with a deletion in V2 loop further stabilises the trimer and also increases the immunogenicity of certain neutralization epitopes. Antibodies against this form reduce viral replication (Srivastava et al., 2003).

Tat-Env

Some studies suggest that extracellular Tat is partially sequestered by heparan sulfate proteoglycans. As a consequence, Tat is concentrated on the cell surface and protected from proteolytic degradation, thus remaining in a biologically active form.

It has been shown that Tat binds the surfaces of both HIV-1–infected and surrounding uninfected cells. Moreoever, there are evidences for a specific interaction between Tat and the gp120 envelope protein, which enhances virus attachment and entry into cells.

Basic science studies and pre-clinical studies are ongoing with the aim to identify and characterize the immunological interaction between Tat and Env, and to identify the role of this interaction, to finally prevent HIV infection and/or progression to AIDS.(Marchio et al 2005)

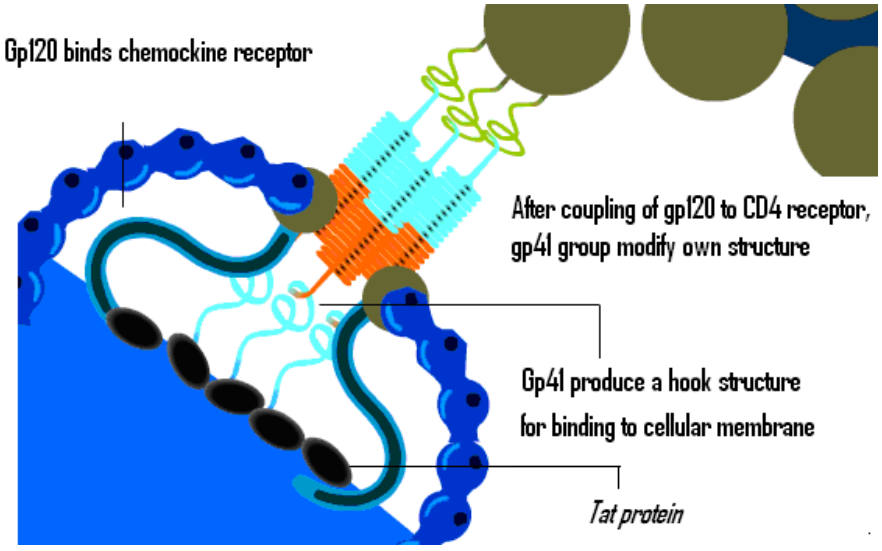

Figure 13: Schematic representation of Tat/Env interaction.

HIV protein-based vaccine

When compared to other viruses, HIV has a number of differences that makes it particularly difficult to fight. Over the past 20 years, most of the efforts in HIV vaccine development have focused on using HIV's Envelope protein (gp120 or Env) in vaccines, in the attempt to induce anti-Env antibodies able to neutralise the infection of the cell by HIV. Theoretically, Env-specific antibodies would prevent entry of the virus into cells. If successful, the vaccine would provide sterilizing immunity, which protects the vaccinated person from becoming infected with HIV.

However, historically, results of Env-based vaccines in pre-clinical and clinical trials have been largely disappointing. In fact, an Env-based vaccine from Vaxgen failed to protect volunteers in phase III clinical trials (Pitisuttithum et al.2006).

Env-based vaccine candidates are believed to have failed because the envelope proteins of the HIV virus mutate rapidly. Because of this characteristic, the immune system is not able to recognize and fight all the variants of the virus. This is similar to what happens with influenza each year, but HIV mutates much faster than influenza.

More recently, other approaches have been developed aimed at inducing T-cell mediated responses against other HIV antigens. However also these approaches failed. An example of this is the recent trial from Merck, based on gag, pol and nef genes, that failed to protect volunteers. These last results come from an international study partly funded by the US National Institutes of Health (NIH).

Regulatory genes, including tat, express proteins soon after infection and are essential for virus replication and pathogenesis. They are also more highly conserved among the different types of the HIV virus found worldwide than are other HIV genes. In addition, Tat is released by infected cells and instructs cells in close proximity to become more prone to infection. These features make the Tat protein a logical candidate for vaccine development.

Tat + Env combination is a vaccination regimen by which individual formulations of Tat and Env proteins will be administered in combination. The separate formulations contain, respectively, Env and biologically active Tat .

Preclinical studies in monkeys indicate that the Tat/Env combination is safe and superior at inducing neutralizing antibodies and, at the same time, increase the breathe of the immune-responses to the single components.

Based on these findings, the scientists are starting Phase I studies with candidate vaccines that combine Tat and Env.[http://www.hiv1tat-vaccines.info/index.php]

AIM OF THE THESIS

Knowledge of the unliganded trimeric Env structure is key point for understanding of viral entry and immune escape and for the design of vaccines to elicit neutralizing antibodies.

The structure of the whole Env complex has remained unsolved till now, due to its complexity and its instability in solution. Structural informations are available only on portion of it, in particular on gp41, for which are available crystallographic data since 1999 (Yang et al. 1999). Crystallographic structures of monomeric gp120 core from SIV (Chen et al. 2005) and from HIV-1, lacking the hypervariable loops and N- and C-termini and complexed with specific ligands (Kwong et al.1998), have been solved. Moreover HIV-1 gp120 core containing the V3 loop structure has been determined (Huang et al.2005).

Most recently a great tool came from the use of cryo-electron tomography, that was employed to determine the three dimensional structure of trimeric Env as complex in situ, on virion particles (Liu et al. 2008; Zanetti et al.2006).

The aim of this work is to try to bridge the gap between the atomic level structures data derived from crystallographic studies and the three-dimensional reconstruction by surface mapping.

By the combined use of chemical modification of cysteine and lysine residues, proteolysis, HPLC and mass spectrometry, we mapped the accessible aminoacids on the surfaces of monomeric gp120 and on trimeric complex of gp140, that is formed by the external domains of the HIV-1 envelope glycoprotein (gp120 and gp41 ectodomain).

From the results useful informations about gp120 structure and how monomers joint together to form trimeric complex are expected.

By the same approach it will be possible to well characterize the interaction surface between Env and Tat protein. This possibly will be a start point for developing a new double protein-based vaccine to employ at prophylactic and therapeutic level.

MATERIALS AND METHODS

gp120 and gp140

Recombinant monomeric Gp120 SF160ΔV2 and trimeric Gp140 SF160ΔV2 were kindly provided by ISS (Istituto Superiore di Sanità).

Counting the number of modified lysine residues of gp140 and gp120 envelope proteins

The reaction of 2,4,6-trinitrobenzenesulfonic acid (TNBS) with amino groups has been used in studying the solvent exposure of lysine residues in gp140 and gp120 envelope proteins.

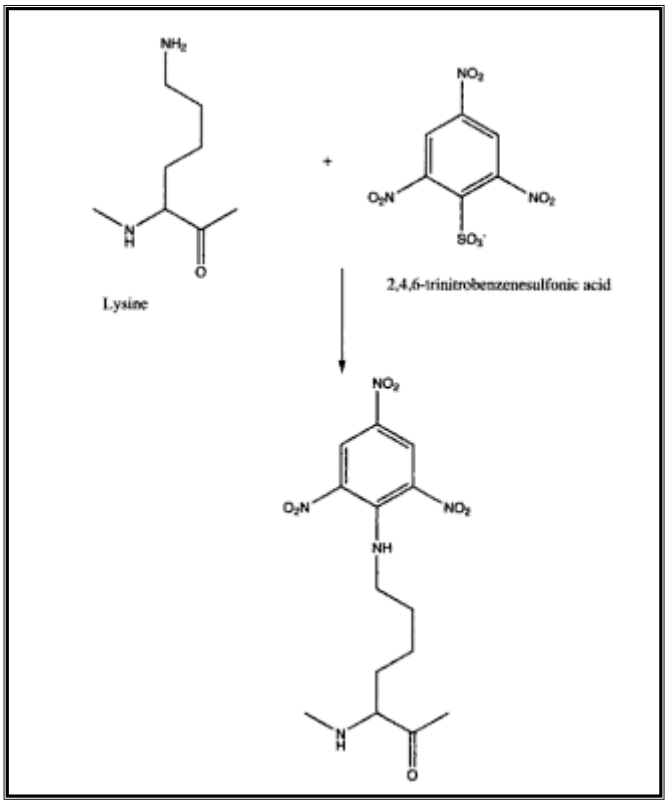

Figure 14: scheme of TNBS reaction

70 µl of gp120 protein or gp140 (0,92 µg / µl) was incubated for minutes at 37°C with 5.0 mM TNBS solution (solved in sodium bicarbonate 0,8 M and NaOH for adjusting pH value at 7.5). Reaction was stopped by adding 2-mercaptoethanol at 37°C for 5 minutes.

Removal of TNBS excess was achieved by use of Microspin™ G-25 Column (Illustra ™ - GE Healthcare).

After freeze drying, the sample was resuspended in a solution of: 8 M urea buffered with 50 mM phosphate buffer, pH 7.8, then iodine-acetate (final concentration 5 mM) and tris-(2-carboxyl-ethyl)- phosphine (TCEP, final concentration 5 mM) were added and the sample was stored for 1 hour at 60°C. The excess of reagents was removed with a Microspin™ G-25 Column (Illustra ™ - GE Healthcare) pre-equilibrated in 20 mM phosphate buffer, pH 7.2.

The reduced and caboxymethylated sample was incubated overnight at 37°C with 2U of N-glycosidase F (Roche) to cleave N-linked carbohydrates.

Then after freeze drying, sample was resuspended in 15 µl of 8 M urea and incubated for 30 minutes at 37°C. Urea concentration in the sample was adjusted to 2 M by adding 50 mM phosphate buffer, pH 7.8.

The sample was digested 5 hours at 37°C with chimotrypsin 5% w/w and the peptides were separated by HPLC

Labelling of cysteine residues of gp120 and gp140 envelope proteins

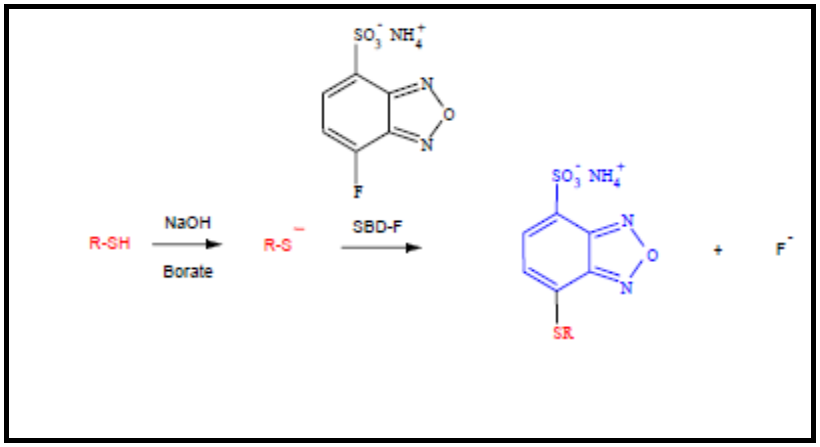

Figure 15: scheme of SBDF reaction

For the labelling of solvent-exposed disulfide was used the reduction by Tris-(2-carboxyl-ethyl)-phosphine (TCEP) and the modification of reduced cysteines by 7-fluorobenzo-2-oxa-1,3-diazole-4-sulfonate (SBD-F).

To 50 µL gp120 protein or gp140 (0,92 µg/µl) envelope protein, SBDF (5.0 mM final concentration) and TCEP (0.22 mM final concentration) were added and the reaction mixture was incubated for 30 min at 37°C in the dark. Reaction was stopped by adding 2-mercaptoethanol at 37°C for 5 minutes. The volume of the reaction mixture was adjusted at 100 µL by adding 50 mM

phosphate buffer, pH 7.0. Removal of SBDF excess was achieved by use of Microspin™ G-25 Column (Illustra ™ - GE Healthcare).

The sample was reduced and carboxymethylated, and treated with -glycosidase F as described above. Digestion was carried out at 5% w/w chymotripsin in 2.0 M urea for 5 h at 37 °C.

HPLC

All runs were carried out on Agilent Technologies 1200 Series HPLC System utilizing an Hypersil C18 reversed-phase analytical column (150 X 4.6 mm, 5 µm particle-size, Agilent), protected with an Alltech C18 guardcolumn (7.5 X 4.6 mm, 5µm particle-size). The detectos was setted at 346 nm for the TNBS-labelled peptides and at 380 nm for the SBDF-labelled peptides.

The samples were eluted at a flow rate of 1. mL/min by gradient of water with 0,1 % Trifluoroacetic acid (TFA) (Sol A) and acetonitrile with 0.09% TFA (Sol B) with the following program

Time	%A	%B
0	100	0
5	100	0
60	40	60
80	20	80
85	20	80

Mass spectrometry (MS)

ESY mass spectrometry was carried out in the department of Chemistry of the University of Ferrara in collaboration with Dott. Alberto Cavazzini e Nicola Marchetti

RESULTS AND DISCUSSION

To verify the better conditions for a reproducible and exhaustive digestion of gp120 and gp140 several proteases and digestion conditions were tested. The results obtained with subtilisin and V8 proteases were scarcely reproducible, and the better results were obtained with chymotripsin in the presence of 2.0 M urea. Despite it is reported that under these conditions some of the protese-sensitive bonds are not hydrolysed, the HPLC profiles were highly reproducible

The labeling of gp120 or gp140 by SBDF was studied at different TCEP concentrations. The lower concentration used was 73.0 μM, nearly stoichiometric with the disulfide bonds present in the proteins, and under these conditions only a very faint labeling occurs. By increasing the TCEP concentration to 0.22 mM (a three fold excess) a significant increase of the extent of labeling was observed, without the appearance of new peaks. A further increase of the TCEP concentration causes an extensive labeling, therefore all the experiments were performed at 0.22 mM TCEP.

The HPLC profile of the chymotrypsin digest of Gp120 labeled with TCEP/SBDF (Fig.16) is indistinguishable from that of the digest of Gp140. This indicates that the disulfide bonds easily accessible to the reagents are not at the trimer interface neither in the C-terminal part of Gp140.

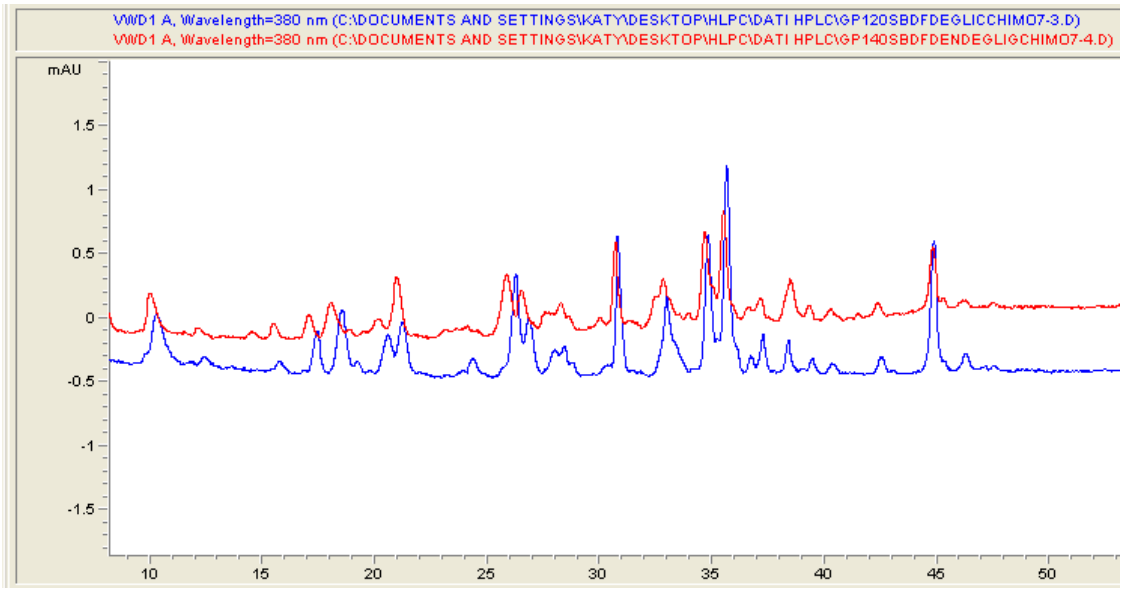

Figure 16: HPLC trace of the chymotryptic digest of Gp120 (blue) and Gp140 (red) labeled with SBDF

Analysis by HPLC/MS of the main peaks allows the identification of ten SBDF-modified peptides, (Table).

Cisteine	Peptide	mass found	mass calculated
53**	**c**asdakay	1026.15	1026.0
118	slkp**c**vkl	1085.42	1085.25
125	tpl**c**vtl	944.13	944.02
155**	kn**c**sf	795.69	795.75
204	n**c**ntsv	834.62	834.76
213	itqa**c**pkv	1057.29	1057.16
226	hy**c**apagf	1062.95	1063.08
255	q**c**thgi	855.86	855.83
390	y**c**nstqlf	1025.9	1026.0
417	tlp**c**rikqi	1269.37	1269.46

Table 1: The mass unit is Da; **, these labeled cysteine residues are not accompanied with the correspondent cysteine in the disulfide bridge (see text)

The data indicate that at least six disulfides are reduced, but two peptides escaped the detection. In fact for the disulfide C53-C73 only the peptide corresponding to the labeled cysteine 53 was found in the major peaks. The same occurred for the disulfide between C130 and C155, where only a labeled peptide corresponding to C155 was found. This unexpected result could be due to different factors. In the native protein the reduction of disulfide could allow local conformational changes resulting in a partial shielding of a cysteine. Otherwise incomplete digestion as well as fragmentation of a peptide in multiple fragments could spread the modified cysteine in several low intensity peaks. In any case if one cysteine is labeled this means that the disulfide is accessible to the reagents.

The reactive disulfides are located in the N-terminal region (C53-C73), in the V1-V2 loops (C118-C213, C125-C204, and C130-C155), between β4 and β8 (C226-C255) and in the V4 loop (C390-C417) between β17 and β19.

Three disulfides appear stable and unlabelled at significant extent under the mild reducing conditions used: C236-C247, located in the loop between β5 and β6; C304-C338, between β12 and β13 closing the V3 loop; C383-C464, between β16 and β22.

Only four of six reactive disulfides can be identified in the three-dimensional structure of Gp120, because all the X-ray structures reported until today are of the core structure, lacking both the N-terminal part and the V1-V2 loops.

The labeling of gp120 and gp140 with TNBS was carried out at keeping the final concentration of the reactive at 5.0 mM, and increasing progressively the incubation time. Up to 5 min of incubation the HPLC pattern is similar, with the height of the peaks increasing by increasing of the incubation time. Longer incubation times cause an extensive labeling, suggesting that also buried residues become accessible

Also the HPLC profiles of the chymotrypsin digest of Gp120 and Gp140 labeled with TNBS are very similar (fig. 17).

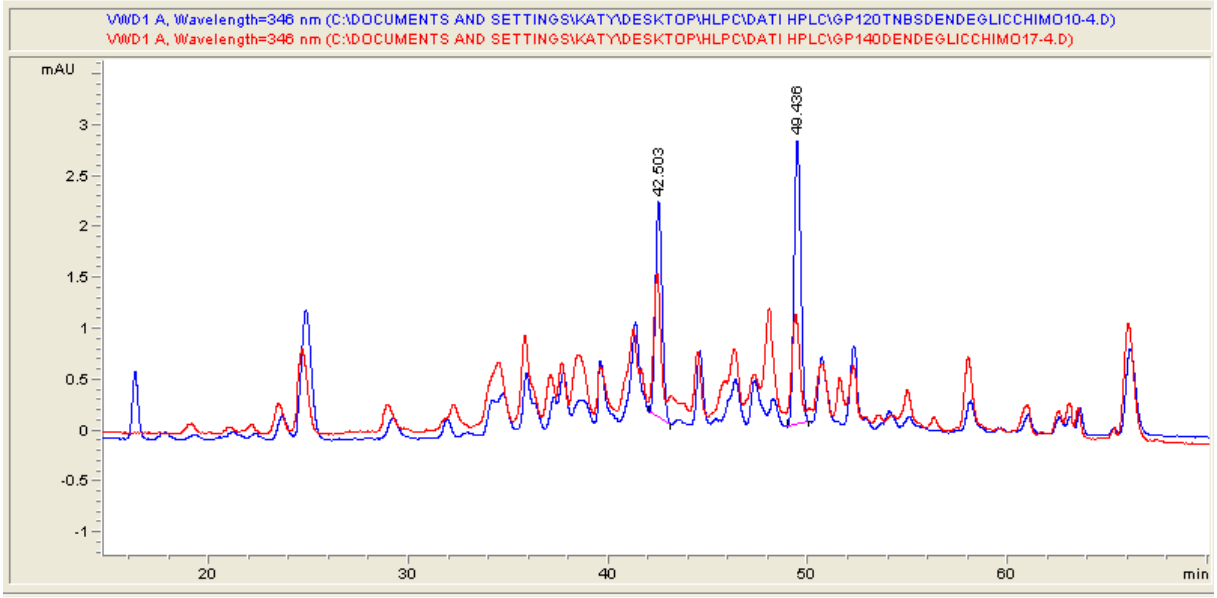

Figure 17: HPLC trace of the chymotryptic digest of Gp120 (blue) and Gp140 (red) labeled with TNBS

Within the major peaks, 18 are identical in both proteins, while four additional peaks are found in Gp140 and on peak, present in Gp120, is absent in gp140. The major common peaks containing labeled lysine residues were identified by HPLC/MS. The labeled peptides found both in Gp120 and in Gp140 are reported in Table 2.

Lysine	peptide	Mass found	Mass calculated
32	ekl	601.62	601.58
45	ygvpvwkeatttl	1678.02	1677.95
120	kl	472.44	472.45
153	drgeikncsf	1439.57	1439.51
159	kvgagkl	1097.04	1097.11
200	gagkli	770.81	770.85
290	tdnakti	975.05	975.0
297	qlkesvei	1158.17	1158.27
350	kqiv	699.76	699.75
355	tkl	573.52	573.57
420	pcrikqi	1128.31	1128.26
431	qevgkam	975.15	975.08
459	trdggkei	1088.19	1088.14
485-487	kykvv *	1091.85	1091.96
490	vki	581.49	581.54

Table 2: *Both mass corresponding to the double labeled peptide (1091.96) and single labeled peptide (848.96) were found.

Only 16 peptides were identified, and six are located in the N-terminal part and in the V1 loop. The single lysine present in the V3 loop was not labeled. K120 and K431 are respectively in β2 and β21, two of the four strands of the sheet involved in the CD4 binding, that are described to undergo a remarkable conformational change in response to CD4 binding. Only four of the lysine identified are highly conserved in different HIV strains, the two already discussed, K120 and K431, plus K350, located in α2, and K487 in β25. All other labeled lysines show a variable degree of substitutions, indicating that these residues are not critical for the structure of the proteins.
All the accessible residues identified are highlighted in the following sequence, where the variable loops V1, V3, V4 and V5 are evidenced. The gag sequence stays for V2.

28 sav

31 eklwvtvyyg vpvwkeattt lfcasdakay dtevhnvwat hacvptdpnp qeivlenvte

91 nfnmwknnmv eqmhediisl wdqslkpcvk ltplcvtlhc tnlknatntk ssnwkemdrg

151 eiknCsfkv gag k

201 lincntsvit qacpkvsfep ipihycapag failkcndkk fngsgpctnv stvqcthgir

261 pvvstqllln gslaeegvvi rsenftdnak tiivqlkesv eincTrpnnn trksitigpg

321 rafyatgdii gdirqahcni sgekwnntlk qivtklqaqf g nktivfkqs sggdpeivmh

380) sfncggeffy cnstqlfnst wnntigpnnt ngtitlpcri kqiinrwqev gkamyappir

440) gqircssnit gllltrdggk eisntteifr pgggdmrdnw rselykykvv kieplgvapt

500) kaissvvqse ks

The position of the labeled residues in the three-dimensional structure of Gp120 is shown in figure 18 and 19. Also in this case the labeled lysine located in the N-terminal and in the V1 loop are not visible on the X-ray structure.

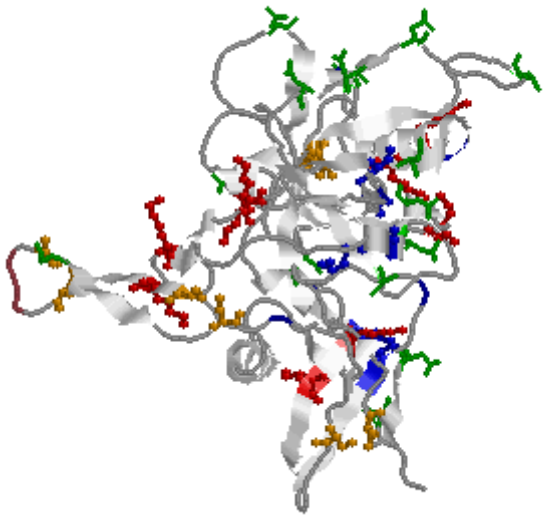

Figure 18: Identification of the labeled residues in the three-dimensional structure of Gp120 from HIV bound to CD4. Reactive lysines are red, reactive cysteines orange, predicted glycosylation sites green, and residue not labeled blue.

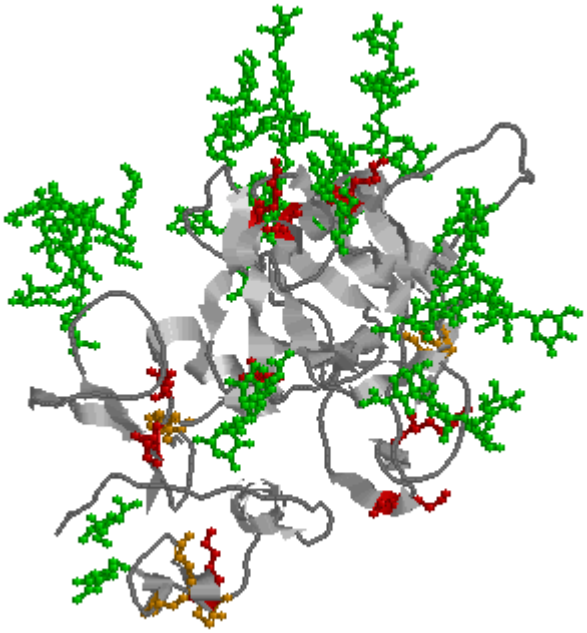

Figure 19: Identification of the labeled residues in the three-dimensional structure of free Gp120 from SIV. Reactive lysines are red, reactive cysteines orange, glycosyl residues green.

A first control of the quality of the data comes from the observation that the sites of interaction between Gp120 and CD4 are all labeled. The protein surface involved in the receptor recognition is obviously exposed, thus an extensive labeling is expected. From the X-ray structure of the complex with CD4 it appears that several part of the Gp120 are involved in the receptor recognition. These parts are β2, β3 and the loop connecting the two strands, and both cysteines and lysines are labeled. The loop between β10 and β11 and the sheets β19, β20 and β21 are equally labeled (Fig 20).

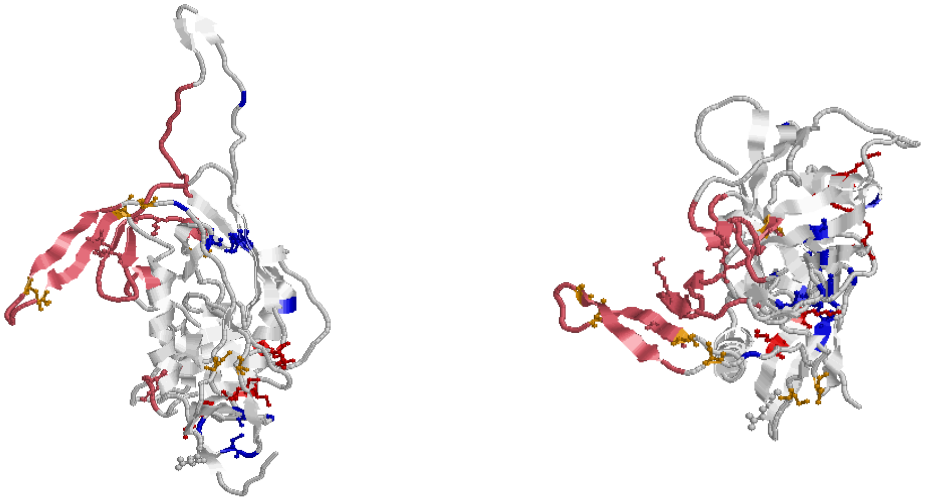

Figure 20: Two view of the CD4 binding site on Gp120 (pink). The other colors are the same of figure 3.

The other major sites of modification are the N-terminal part and the V1 loop, both absent in the three-dimensional structure, the V5 loop, and the sheet β25. The V4 loop does not present neither cysteines or lysines, so it is impossible to know whether is exposed. The V3 loop present a lysine, but, as already pointed out, it is not labeled. This suggests that the V3 loop is, at least partially, shielded from the solvent.

An examination of the overall structure evidences large parts of the molecule not accessible to the reagents. In fact the reactive residues appear clustered mainly in two parts: the N- and C- terminal part, that are supposed to face the Gp41 and the viral membrane, and the external part, where is located the CD4 binding site.

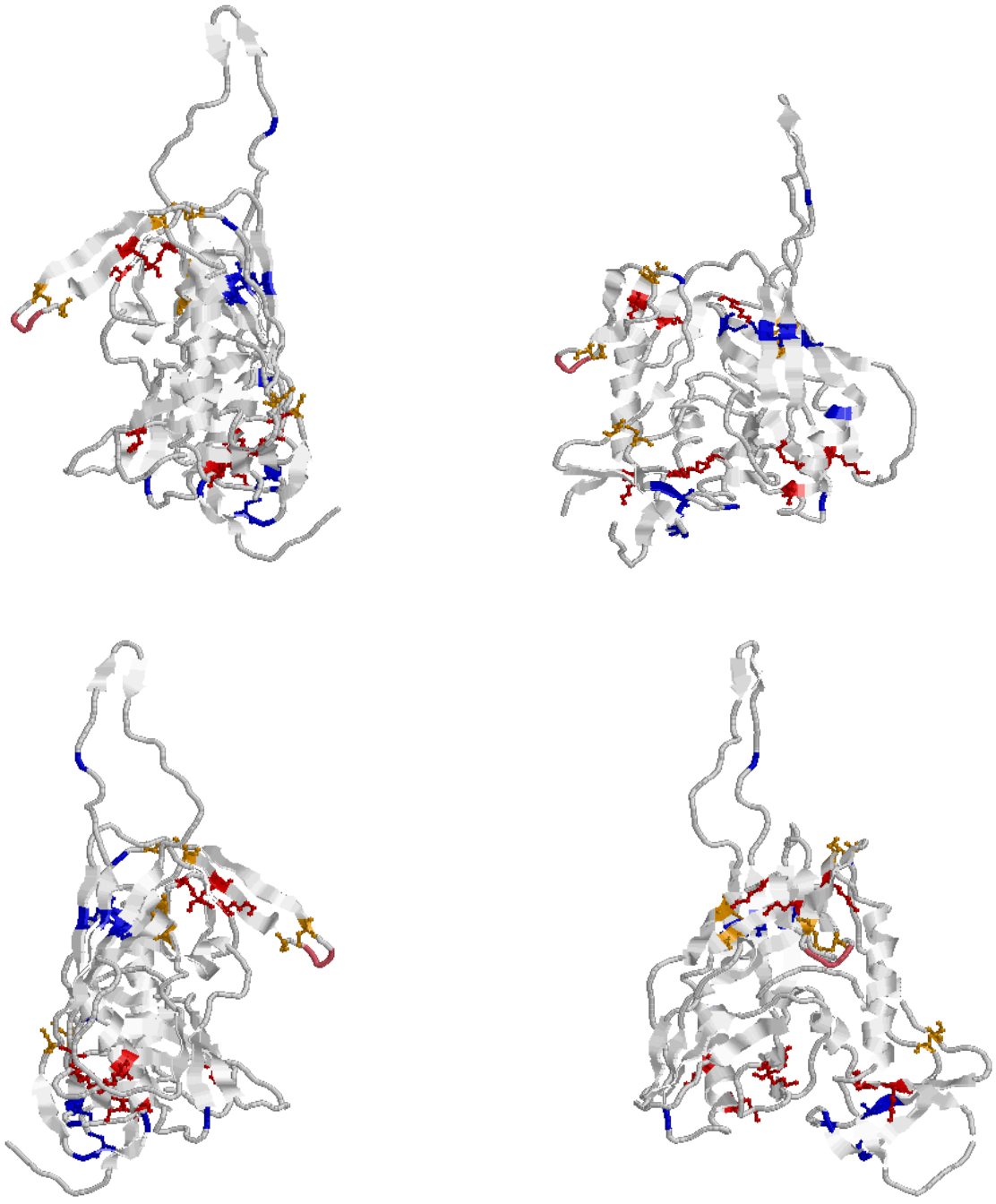

Figure 21:View of the reactive/non reactive residues. Each figure is rotated by 90°

Despite the distribution of reactive residues on the three-dimensional structure is not uniform, a significant restrain can be imposed in the building of the trimer structure. However there are still several uncertainty, due to the lack of a significant part of the protein in the X-ray structure. For

example about 50 amino acids are lacking at the N-terminal part. These amino acid are solvent exposed, and could shield some part of the molecule.

Nevertheless some preliminary conclusion can be drawn. When the X-ray structure of Gp120 was fitted into the shape of the Env trimer, obtained by cryo-electron tomography (Zanetti et al, PLOS 2006), two possible conformations were found: one with the V3 loop exposed to the solvent, and another with the loop buried. Surface labeling data suggest that the model with V3 loop buried is more consistent.

PART II:
role of hexose-6-phosphate mutarotase from *Trypanosoma brucei* in oxidative stress

INTRODUCTION

Parasites

Parasitic protozoa infect hundreds of millions of people every year and are some of the most important causes of human misery. Trypanosomes are a group of kinetoplastid protozoa distinguished by having only a single flagellum. Members of this group parasitize virtually all animal groups as well as plants and insects. Three distinct kinetoplastids cause human disease: various species of *Leishmania* cause the Leishmaniasis, *Trypanosoma cruzi* and *Trypanosoma brucei* are respectively , the causative agent of Chagas Disease and African sleeping sickness. All three are parasites of the blood and/or tissues of the human host and are transmitted by arthropod vectors.

Currently the Leishmaniasis, prevalent in four continents, are considered to be endemic in 88 countries, 72 of which are developing countries. It's transmitted by the bite of certain species of sand fly.Occurring in several forms, the disease is generally recognized for its cutaneous form which causes non-fatal,disfiguring lesions, although epidemics of the potentially fatal visceral form cause thousands of deaths.

Chagas disease occurs exclusively in Latin America in particular in the poor, rural areas of Mexico, Central America, and South America; it's transmitted via faeces of a bug belonging to the family Triatominae.

The symptoms of Chagas disease vary over the course of the infection. In the early, acute stage, symptoms are mild and usually produce no more than local swelling at the site of infection. As the disease progresses, over the course of many years, serious chronic symptoms can appear, such as heart disease and malformation of the intestines. If untreated, the chronic disease is often fatal. Current drug treatments are generally unsatisfactory; available medications are highly toxic and often ineffective, particularly those used to treat the chronic stage of the disease.

Human African Trypanosomiasis

Human African Trypanosomiasis (HAT), also known as Sleeping sickness, is caused by *T. brucei*. It's transmitted to humans by tsetse fly (Glossina Genus) bite which have acquired their infection from human beings or from animals harbouring the human pathogenic parasites. Although epidemics of sleeping sickness were more rampant in the past, the most recent World Health Organisation (WHO) estimates put 60 million people at risk of HAT today with approximately 500,000 people currently with infections. The disease is discontinuously spread over 9 million square kilometers and affects populations across 37 sub-Saharan countries.

H A T takes two forms, depending on the parasite involved.

- ✓ *T. brucei gambiense (T.b.g.)* is found in west and central Africa. This form represents more than 90% of reported cases of sleeping sickness and causes a chronic infection. A person can be infected for months or even years without major signs or symptoms of the disease. When symptoms do emerge, the patient is often already in an advanced disease stage when the central nervous system (CNS) is affected.
- ✓ *T. brucei rhodesiense (T.b.r.)* is found in eastern and southern Africa. This form represents less than 10% of reported cases and causes an acute infection. First signs and symptoms are observed after a few months or weeks. The disease develops rapidly and invades the central nervous system.

A third sub-specie, *T. brucei brucei*, does not infect humans, but it causes a disease called Nagana in native antelopes, domestic livestock and other African ruminants with a high economic impact for local agriculture.

There are two stages in sleeping sickness; the early stage refers to the hemolymphatic infection, and the late stage refers to infection of the CNS.

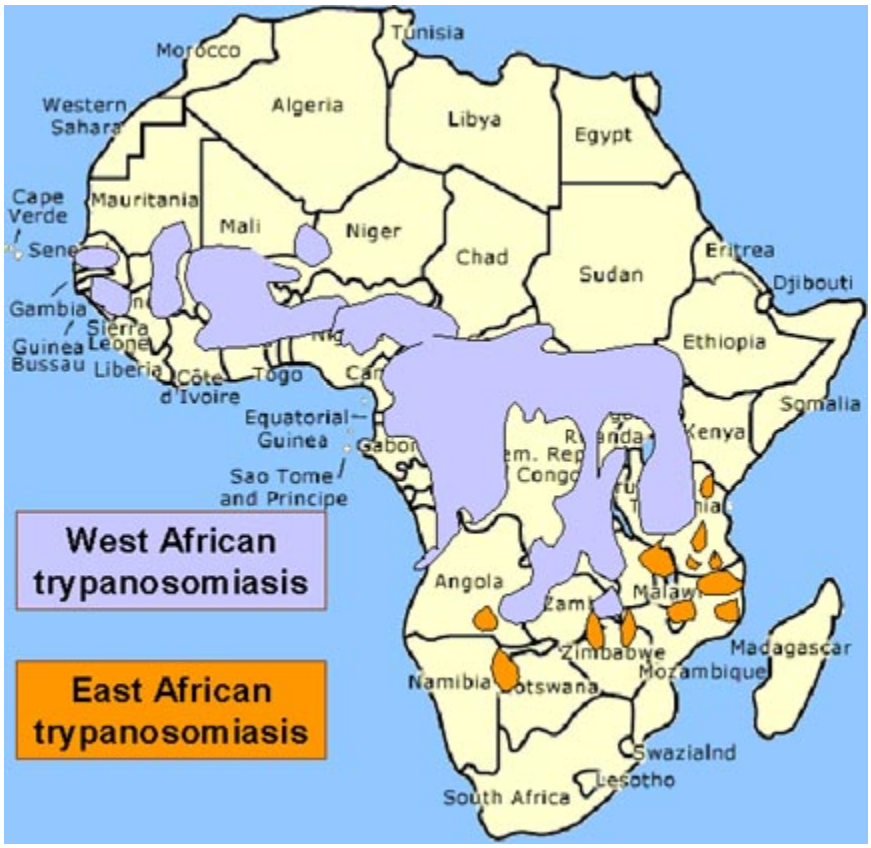

Fig. 1: Distribution of Human African Trypanosomiasis

The development of late stage sleeping sickness may not occur for decades in West African sleeping sickness, and a patient may only suffer mildly from fatigue due to the occasional rises of parasites in the blood. However, East African sleeping sickness is far more virulent, and can develop into late stage disease within weeks. Although symptoms and signs associated with nervous system involvement are varied for both East and West African sleeping sickness; advanced disease epileptic attacks, maniacal behavior, somnolence and coma are some typical late stage symptoms. Both treatment options and survival rates are drastically reduced once the trypanosomes infect the CNS.

There is no vaccine available to prevent this disease and the possibility of developing one is still very remote, due to the periodic antigenic variation of the Variable Surface Glycoprotein (VSG) coat.

Only four parental drugs are registered for the treatment of Human African Trypanosomiasis: pentamidine, suramin, melarsoprol and eflornithine. Three of them were developed over 50 years ago. All of the current therapies are unsatisfactory for various reasons, including unacceptable toxicity, poor efficacy, undesirable route of administration (parental only) and drug resistance.

Pentamidine and suramin are used in the first or early stage of *T.b.gambiense* and *T.b. rhodesiense* infections, respectively. Melarsoprol is used in the second or advanced stage of both form of the disease and eflornithine is only used in the second stage of the *T.b.gambiense* infections since it has been found not to be effective in the disease due to *T.b rhodesiense*.

This lack of effective, safe and affordable pharmaceuticals to control this disease, that cause high mortality and morbidity among poor people in the developing countries, underlines the urgency to find new drugs.

The pharmaceutical industry argues that research and development is too costly and risky to invest in low-return neglected diseases; public and private initiatives have tried to overcome this market limitation through incentive packages and public-private partnerships. The lack of drug research and development for "non-profitable" infectious diseases will require new strategies. No sustainable solution will result for diseases that predominantly affect poor people in the South without the establishment of an international pharmaceutical policy for all neglected diseases. But in recent years research has produced many data to identify enzymes, other proteins and peculiar organelles as potential drug targerts

The *Trypanosoma brucei*

African trypanosomes are extracellular organisms, mono-flagellated protozoa with a complex life cycle involving an obligate change between an insect and a mammalian host.

T. b. gambiense and *T. b. rhodesiense* are morphologically indistinguishable, measuring 25-40 μm in length. Infection in the human host begins when the infective stage, known as the metacyclic stage, is injected intradermally by the tsetse fly. The organisms rapidly transform into blood-stage trypomastigotes (long, slender forms), and divide by binary fission in the interstitial spaces at the site of the bite wound.

Trypanosomes have a single specialized mitochondrion in which all of the DNA is localized in the kinetoplast, which is a part of mitochondrion adjacent to the flagellar pocket. Kinetoplast DNA or kDNA exists in two forms: mini-circles and maxi-circles. Mini-circle DNA encodes guide RNAs that direct extensive editing of RNA transcripts post-transcriptionally. Maxi-circle DNA contains sequences that, when edited, direct translation of typically mitochondrially-encoded proteins.

kDNA undergoes repression and activation so that the trypanosome can switch its pattern of respiration to match its host's energy source.

Cellular features of the trypanosomes include a single flagellum that emerges from the flagellar pocket, the region to which endo- and exocytosis is limited.

The nuclear DNA is organized in separate chromosomes where the genes are organized in long, polycistronic transcription units. The genes are separated by only a few hundred base pairs and are without introns. The polycistronic precursor transcripts are processed into mRNAs by trans splicing, in which each transcripts obtains a capped leader of 39 nucleotides and a 3' poly A tail. In *T.brucei* only four promoters are known, one is responsible for transcription of spliced leader RNA, one for rRNA and the other two direct transcription of VSG and Procyclin.

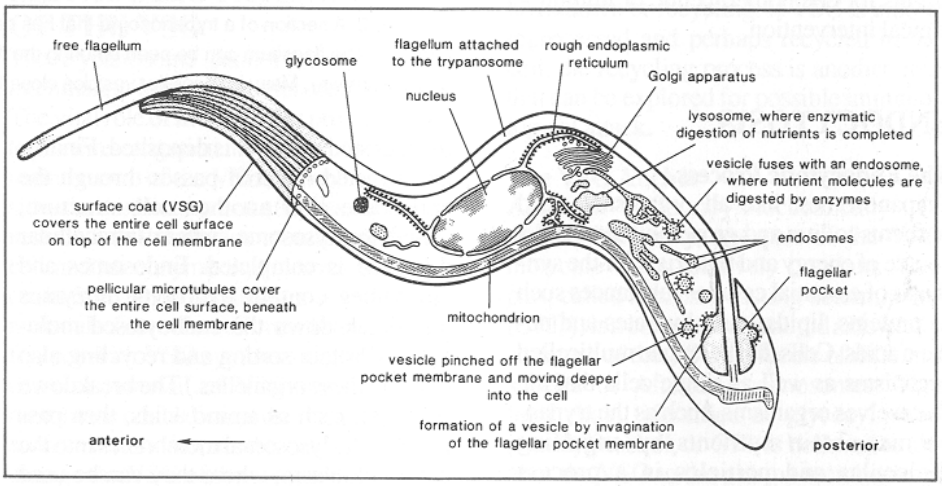

Fig. 2: Schematic rappresentation of *T.brucei*

The surface of the trypanosome is covered by a dense coat of Variable Surface Glycoprotein (VSG), which allows persistence of an infecting trypanosome population in the host.

Periodic antigenic variation allows variants expressing a new VSG coat to escape the specific immune response raised against the previous coat.

Sequencing of the *T. brucei* genome has revealed a huge VSG gene archive, made up of thousands of different VSG genes. It is estimated up to 10% of the *T.brucei* genome may be made up of VSG genes or pseudogenes. All but one of these are 'silent' VSGs, as each trypanosome expresses only one VSG gene at a time. VSG is highly immunogenic, and an immune response raised against a specific VSG will rapidly kill trypanosomes expressing this VSG. However, with each cell division there is a possibility that one or both of the progeny will switch expression to a silent VSG from the archive. The frequency of such a switch has been measured to be approximately 1:100. This new VSG will likely not be recognised by the specific immune responses raised against previously expressed VSGs. It takes several days for an immune response against a specific antigen to develop, giving trypanosomes which have undergone VSG coat switching some time to reproduce unhindered. Repetition of this process prevents extinction of the infecting trypanosome population, allowing chronic persistence of parasites in the host. The clinical effect of this cycle is successive 'waves' of parasitaemia (trypanosomes in the blood).

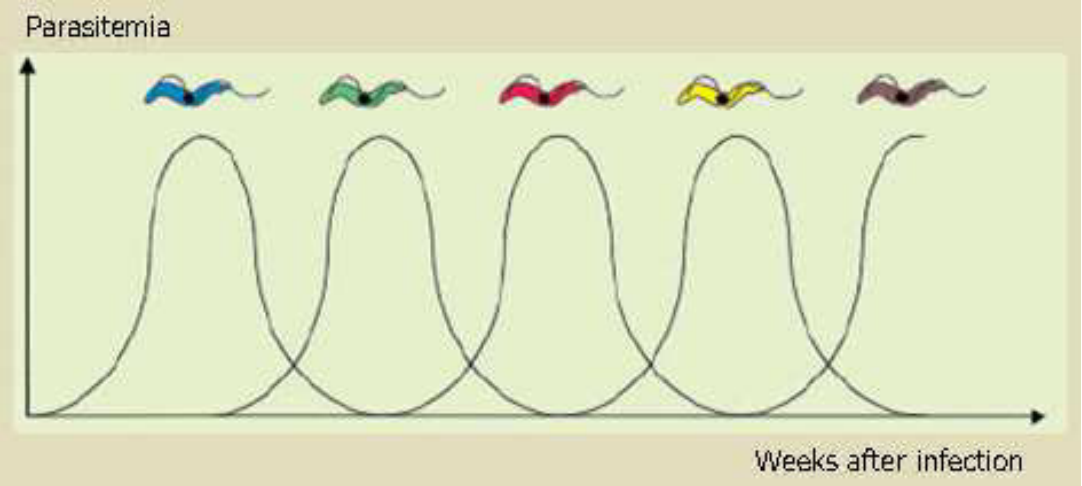

Fig. 3: Sinuous variation in parasite population due to immune evasion strategies of the parasite

Life cycle

By taking a blood meal metacyclic trypomastigotes in the saliva of the tsetse fly are inoculated to the mammalian host (e.g. humas, cattles) causing some days later a local inflammation reaction with a typical erythema. Swelling of lymph nodes occurs at the site of infection and trypanosomes undergo cell cycle re-entry and a morphological change to proliferative, long-slender bloodstream trypanosomes (or trypomastigotes) followed by asexual multiplication by binary division.

Finally the trypomastigotes are released via lymph vessels and lymph nodes into the blood circulation.

A fluctuating fever occurs in the patient, synchronic with the parasitaemia. When density of trypanosome increases in the blood, transformation occurs to non-proliferative short stumpy forms (indicated by cell cycle arrest, raising mitochondrial activity and resistance to lysis by antibody). The population of long-slender, short stumpy and transition stage forms is being described as pleomorphic. The short-stumpy trypanosomes are ready for re-transmission to the tsetse fly.

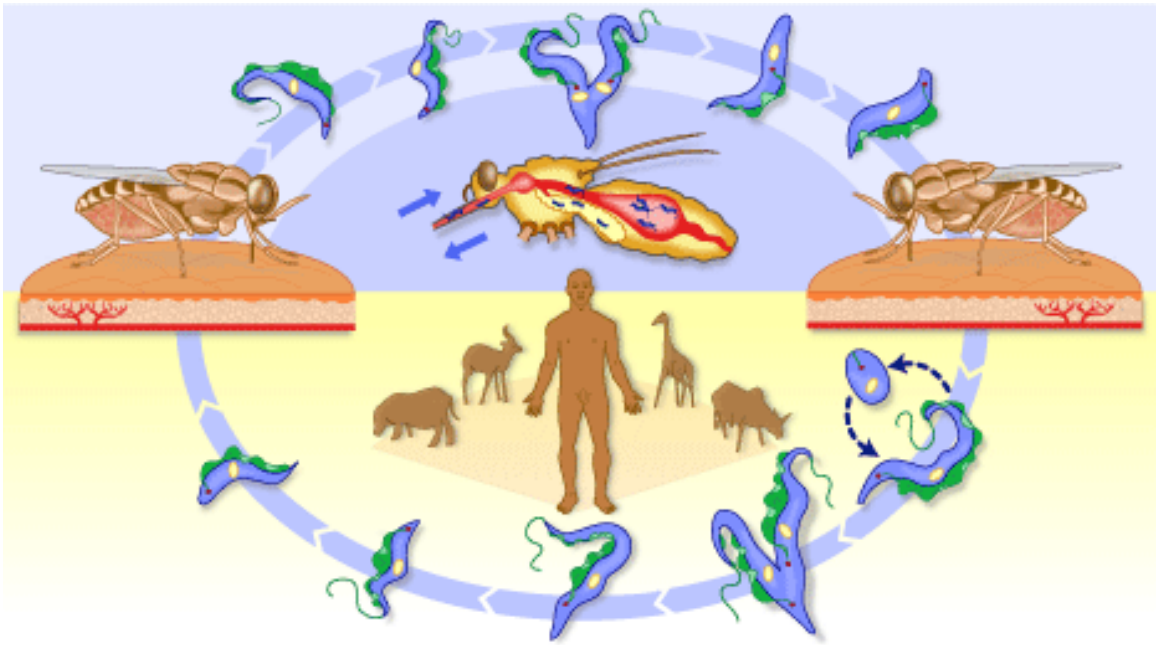

Fig. 4: *T. brucei* life cycle (WHO)

Only weeks or months after infection parasites cross the blood-brain barrier and invade the CNS, where they cause a chronic encephalopathy. Symptoms are headaches, disorder of the sleeping rhythm (therefore the disease has got the second name “sleeping sickness”), apathy, somnolence and in the latest stage coma and lead finally, if untreated, to death of the patient.

A physical characteristic of the fist stage of the disease is a swelling of lymph nodes in the neck, known as “Winterbottom sign”. The diagnosis however is complex and elaborate, the therapy complicated and expensive and can in addition be perilous for the patients.

When re-entered in an insect host short-stumpy trypanosomes enter the fly’s midgut. Shortly afterwards they transform into procyclic trypomastigotes and reproduce asexually by binary fusion. Then they move to the anterior part of the midgut and elongate to produce mesocyclic trypomastigotes that will migrate to the salivary glands to quickly develop into epimastigotes (Van Den Abbeele et al., 1999), attached by their flagella to the wall of the glands.

Energy metabolism

Like many organisms, trypanosomes have to perform metabolic adaptation to highly varying environmental conditions encountered during their complex life cycle, including the transmission

between an insect and a mammalian host. In both organisms they transit through different parts of the body, each time being exposed to different environmental conditions.

Trypanosomes feed by taking up nutrients, through their plasma membrane, from the body fluids of the host, by using specific nutrient transporters and by endocytosis.

The major human pathogenic stage of *T. cruzi*, the amastigotes which reside in the cytoplasm of the host cells, bases its energy metabolism largely on carbohydrates being provided as freely accessible sugar phosphates and *Leishmania* amastigotes, the pathogenic stage residing in phagolysosomes of macrophages, rely more on fatty-acid and amino-acid metabolism. In contrast, bloodstream form *T. brucei* is up taking glucose as energy substrate from the fluids of its host.

The metabolism in different life-cycle stages differs considerably. The BF is completely dependent on glycolysis for its ATP supply. In contrast, glycolysis is less important in PF trypanosomes, which have a more oxidative form of metabolism with their well-developed mitochondrion.

Probably in order to refine their adaptation capacity trypanosomes have developed a special form of metabolic compartmentalization in which glycolysis features prominently. Whereas in most organisms glucose metabolism is taking place exclusively in the cytosol, the larger part of glycolysis in trypanosomatids takes place in specialized organelles hence called glycosomes (Hannaert et al., 2003, Michels et al., 2006). This unique form of glycolysis compartmentalization was originally found in *T. brucei* (Opperdoes and Borst, 1977), but was subsequently also discovered in *T. cruzi* and various *Leishmania* species, as well as parasites of other vertebrates, invertebrates and plants, all belonging to the Kinetoplastida. Glycosomes may comprise up to 90% of its protein content as glycolytic enzymes and bloodstream trypanosomes contain approximately 65 of these organelles.

These organelles contain, in addition to the enzymes for the first seven glycolytic steps (Fig 5), the enzymes of the oxidative branch of the pentose phosphate pathway (PPP).

Despite their prominent glycolytic function and the lack of catalase, glycosomes belong to the peroxisome family, taking in account the single phospholipid bilayer, the fact that they do not contain DNA and the similar process of biogenesis involving homologous proteins, the so called peroxins. Proteins imported into glycosomes and peroxisomes require a peroxisome-targeting signal (PTS).

This compartmentalization of glycolysis in the glycosome seems to be important for metabolic homeostasis. Activities of glycolytic enzymes such as hexokinase (HK) and phosphofructokinase which are normally highly regulated seem to be unregulated in trypanosomes (Nwagwu and Opperdoes, 1982). In yeast mutants it has been shown that absence of active regulation of these

enzymes may lead to unrestricted accumulation of glycolytic intermediates which could be highly toxic for the cell.

Mathematical modelling showed that improper compartmentalization of glycolytic enzymes in trypanosomes would also cause uncontrolled accumulation of hexose 6-phosphates, because the kinases are responding to the glycosomal ATP/ADP ratio that is usually low but the enzymes would sense the high cytosolic ATP/ADP ratio in the case of defect in glycosomes or improper compartmentalization and consequently they would be activated without being restrained by the product for which the trypanosome enzymes are not sensitive. Indeed, experimentally it has been confirmed that correct compartmentalization of glycolytic enzymes inside glycosomes is essential for the survival of bloodstream form *T. brucei* (Guerra-Giraldez et al., 2002). Abundance of glucose in the bloodstream and a high rate of aerobic glycolysis (with pyruvate as end product) allow bloodstream form *T. brucei* to proliferate rapidly. ATP is produced exclusively by glycolysis: two molecules ATP per molecule glucose are consumed.

Glycolysis in trypanosomes is considered a validated drug target because these parasites are completely dependent on the conversion of glucose into pyruvate for their ATP supply when living in the mammalian bloodstream (Bakker et al., 2000, Verlinde et al., 2001). The seven enzymes involved in the conversion of glucose into 3-phosphoglycerate are present inside the glycosomes, while those catalyzing the last part of the pathway are localized in the cytosol (Fig. 5) (Opperdoes and Borst, 1977).

Knockdown of the expression of glycolytic enzymes by RNA interference (RNAi) resulted in death of the parasites (Albert et al., 2005).

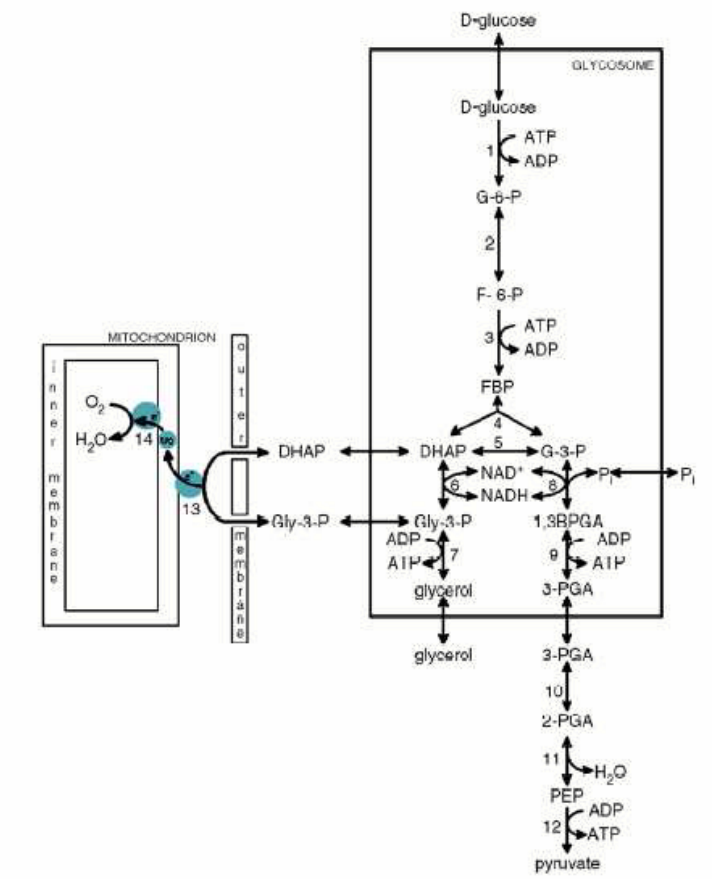

Fig. 5 : Schematic representation of glycolysis in the bloodstream form of *T.brucei*. (Under aerobic conditions, glucose is converted into pyruvate. Under anaerobic conditions equimolar amounts of glycerol and pyruvate are produced) (Michels et al., 2006)

The PPP is also very important for trypanosomes since it provides NADPH, required for many biosynthetic and detoxification reactions and active in protection against oxidative stress, and ribose, essential for nucleotide biosynthesis. Enzymes of this pathway have a dual localization: in the cytosol and in glycosomes (Duffieux F et al., 2000, Michels P.A. et al., 2006). Both the dehydrogenases of the PPP are considered valid drug targets against HAT, indeed RNAi experiments have shown that they are essential for growth of *T. brucei* bloodstream forms (Barrett et al., 2002, Cordeiro et al., 2009) Inhibitors of 6-phosphogluconate dehydrogenase (6PGDH) have been found with trypanocidal activity (Hanau S. et al., 2004) and 6PGDH inhibition leads to accumulation of 6-phospho-gluconate, which is a competitive inhibitor of GPI in glycolysis (Marchand M. et al., 1989).

Defence against oxidative stress in Trypanosomes

Throughout their life cycle trypanosomes are exposed to oxidative stress imposed by reactive oxygen species (ROS) derived from its own aerobic metabolism, and from the host immune response.

In nearly all organisms, glutathione and glutathione reductase are involved in the maintenance of the intracellular reducing environment. This is important for the reduction of disulphides, the detoxification of hydroperoxides and the synthesis of DNA precursors (Schirmer et al., 1987, Penninckx and Elskens, 1993). Kinetoplastid protozoa, highly sensitive to oxidative stress caused by reactive oxygen species, lack glutathione reductase (Fairlamb and Cerami, 1985) and many of the functions ascribed to glutathione and glutathione reductase appear to have been taken over by N1,N8-bis(glutathionyl)spermidine (trypanothione) and trypanothione reductase (TRYR) (Fairlamb et al., 1985; Fairlamb and Cerami, 1992).

Trypanothione is kept reduced by trypanothione reductase using NADPH and the major source of this reduced coenzyme seems to be the PPP.

An other important enzyme seems to be lipoamide dehydrogenase producing free thiols with antioxidant power in the form of dihydrolipoate. In leishmania 4-mercaptohistidine (ovothiol A) is an other strongly low-molecular-weight thiol (Krauth-Siegel and Schoneck, 1995).

Anomeric specificity of enzymes

α- and β-anomers of aldose sugars can spontaneously interconvert. D-Glucose and D-glucose 6-phosphate (Glc6P) are examples of hexose carbohydrates that, in solution, undergo spontaneous interconversion between α and β anomeric forms. This reaction, known as mutarotation, happens at slow rates when compared to the corresponding enzyme-assisted process. Rate constants for spontaneous mutarotation of glucose and glucose 6-phosphate are 0.015 min^{-1} and 0.09 min^{-1}, respectively (Livingstone et al., 1977). In equilibrated solutions of D-glucose and D-Glc6P, the ratio of α to β anomer is 33:66 and 20:80, respectively.

Several enzymes of carbohydrate metabolism show different levels of anomeric selectivity, which can vary from a moderate preference to full specificity. Hexokinases have a preference for α-glucose; yeast glucose-6-phosphate dehydrogenase (G6PDH) is specific for β-D-Glc6P; phospho-glucose isomerase (PGI) is specific for α-Glc6P while it is specific for β-D-fructose-6-phosphate,

both as a substrate and a product, and has an anomerase-like activity for both these hexose-6-phosphate, Glc6P and fructose-6P (Salas et al., 1965, Willem et al, 1992))(Scheme 1 and Fig. 6).

Very recently, the crystal structure of the *T.cruzi* ATP-dependent glucokinase (GlcK) complexed with glucose was determined (Cordeiro et al., 2007). Whereas in all available exokinase (HK) crystal structures, glucose was found as an α-anomer, in line with the known general preference of HKs for this anomer (Malaisse, 2003), it could be concluded from the electron density of the *T. cruzi* GlcK structure that the bound D-glucose was in the β-configuration.

Kinetic assays with α- and β- D-glucose further confirmed a moderate preference of the *T. cruzi* GlcK for the β-anomer (Cordeiro et al., 2007). The reason for the presence of a GlcK in these parasites (also in *Leishmania major*, but absent from *T. brucei*, (Caceres et al., 2007)) in addition to a HK, is not clear yet.

Glycolysis is, according to the literature, highly specific for α-sugars, whereas the PPP would be highly specific for β-sugars.

Notably in Trypanosomes, the first enzyme specific of each pathway, following the shared HK, displays high anomeric specificity: PGI for α-Glc6P, G6PDH for β-Glc6P. It could therefore be imagined that the GlcK of *T. cruzi* and *L. major* serves primarily to feed the PPP, and HK the glycolytic pathway.

If, however, *T. brucei* has only a HK, but no GlcK, it would need an additional enzyme, to get the β-Glc6P for its PPP, implicated in this step.

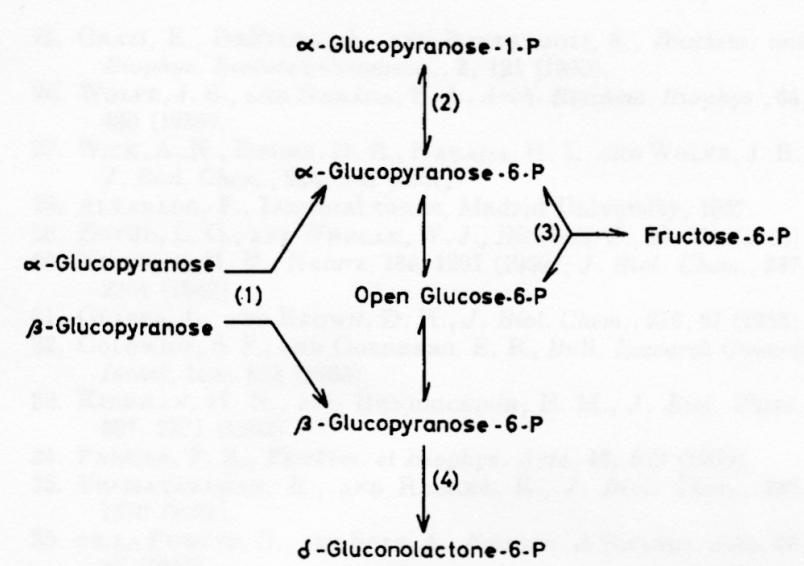

SCHEME 1. Anomeric specificity in glucose-6-P metabolism. *1*, hexokinase; *2*, phosphoglucomutase; *3*, glucose phosphate isomerase; *4*, glucose-6-P dehydrogenase.

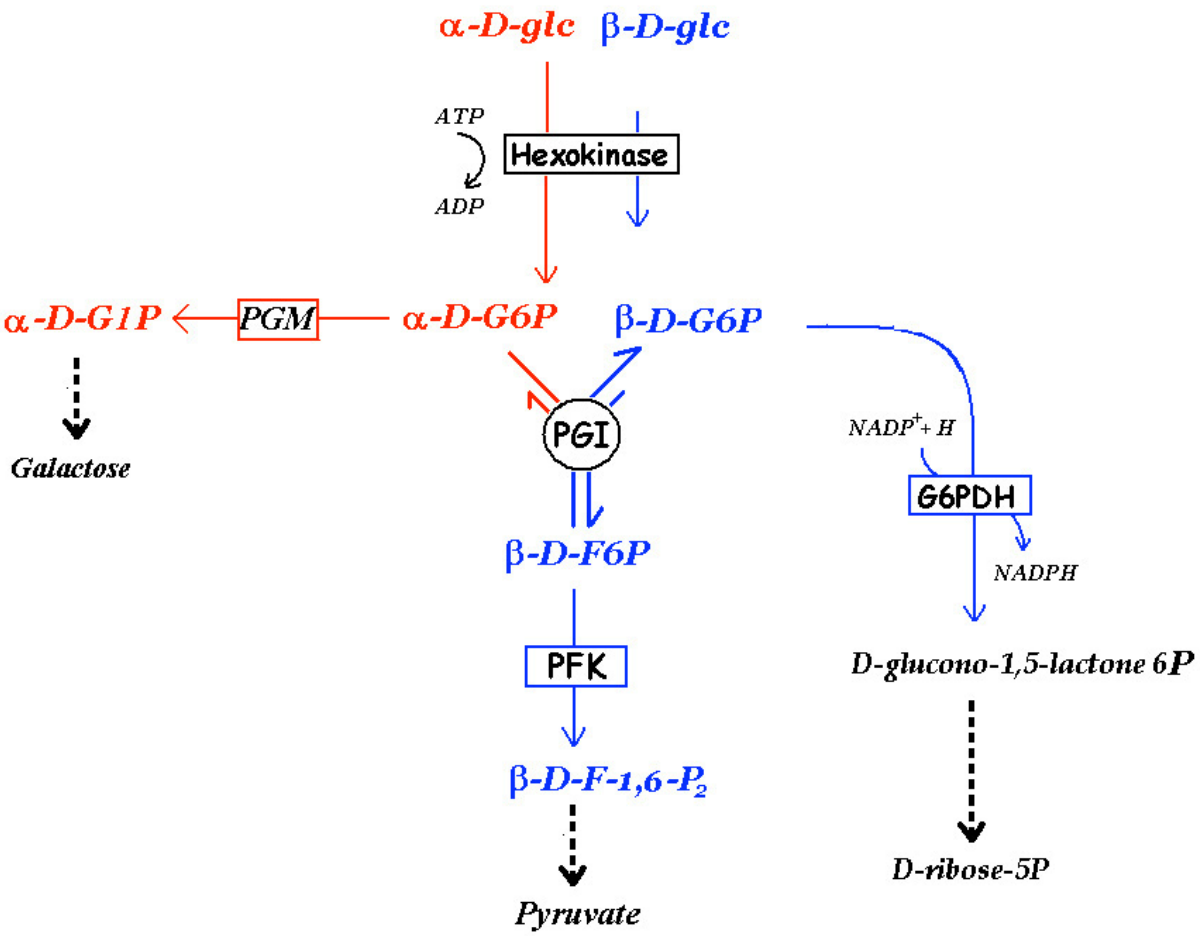

Fig. 6 : Schematic representation of anomeric specificity of enzymes involved in the metabolic cross-road at the level of glucose-6P. PGM, phosphoglucomutase, PGI, glucose phosphate isomerase, PFK, phosphofructokinase, G6PDH, glucose-6-P dehydrogenase

Hexose-6-phosphate mutarotase

Recently determined structure-based data give evidence that the *S. cerevisiae ymr099c* gene product exhibits hexose-6-phosphate mutarotase (H6PM) activity on Glc6P, galactose 6-phosphate (Gal6P) and mannose 6-phosphate (Man6P) (Graille et al., 2006). This study was based on the previous finding of an unidentified enzyme with Glc6P mutarotase activity (Wurster and Hess, 1972).

Recently the genome sequencing project of *T. brucei* (927 strain) (Berriman et al., 2005) has been completed and provides a great tool to find out more about the complexity of metabolic pathways. Using the yeast H6PM sequence, a homologous sequence could be detected in the databases of *T. cruzi*, *L. major* and *T. brucei.*

In a previous study of comparative proteomics of bloodstream and procyclic *T. brucei* glycosomes various proteins have been identified by nanoLC-MS/MS, which are annotated in GeneDB as hypothetical proteins. Among those a protein (GeneDB accession number Tb927.4.1360) found in procyclics, that the proteomics researchers annotated as 'aldose-1-epimerase-like' and with a PTS1 localisation signal could be detected (Colasante et al., 2006).
Indeed, an aldose-1-epimerase motif was predicted by Pfam database. However, because of its similarity with yeast YMR099c, with residues involved in the 6-phospho group binding conserved, it seems likely that it is a H6PM, suggesting that mutarotation of sugar phosphates plays an important role in *T. brucei* metabolism to provide the PPP with its substrate.
The low spontaneous mutarotation rates and the anomer selectivity of key enzymes of sugar metabolism highlight the importance of mutarotases to support fast metabolic fluxes.

State of the art on H6PM from *T. brucei*

The *T. brucei* sequence homologous to yeast H6PM, was cloned and expressed in *E. coli* (Moebius, thesis). It appears that *T. brucei* H6PM exists as a monomer of 32.5 kDa and a dimer of 63,2 kDa. The dimeric form is much more concentrated, but there is decomposition of the dimeric state over time.
The overall similarity between the yeast and *T. brucei* sequence is up to 31.2 % and the active site residues and other motifs for the binding of the hexose 6-phosphate molecule and catalysis by the yeast enzyme are found to be conserved in the trypanosomatid sequence (Fig. 7). Site-directed mutagenesis could show that in *L. lactis* galactose mutarotase, His170 and Glu304 play the role of catalytic acid and base, respectively (Thoden et al., 2003). In the yeast Glu203 may act as a general base through deprotonation of the anomeric O1 hydroxyl group while His159 as the acid by protonating the O5 sugar ring oxygen. Besides the homology in residues for the catalytic mechanism, there are also especially two arginines ("arginine clamp" formed by Arg57 and Arg86, yeast numbering) present in the trypanosomatid sequence important for accession and binding of the phosphate group of the hexose 6-phosphate molecule. This feature makes the H6PMs differ from the homologous aldose 1-epimerases acting on hexoses normally and not containing positive side chains in the needed conformation to host a phosphate group.
Regarding the global three-dimensional structure the H6PM sequence presents the motif of aldose-1-epimerase like galactose mutarotase, which is also present in yeast H6PM. These enzymes are beta proteins with a supersandwich fold (Fig. 8, Graille et al. 2006).

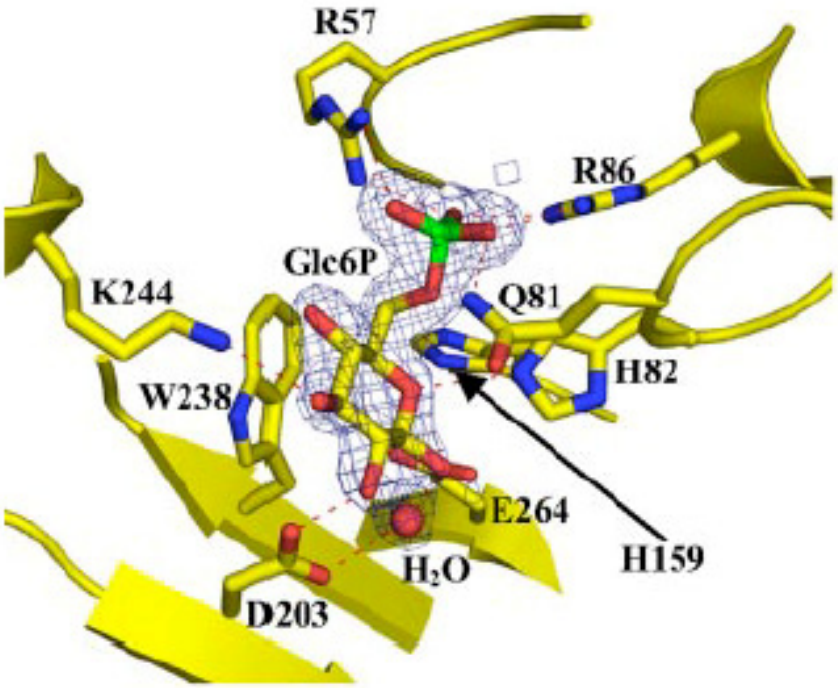

Fig. 7: Complex of yeast PGM bound to β-glucose 6P.

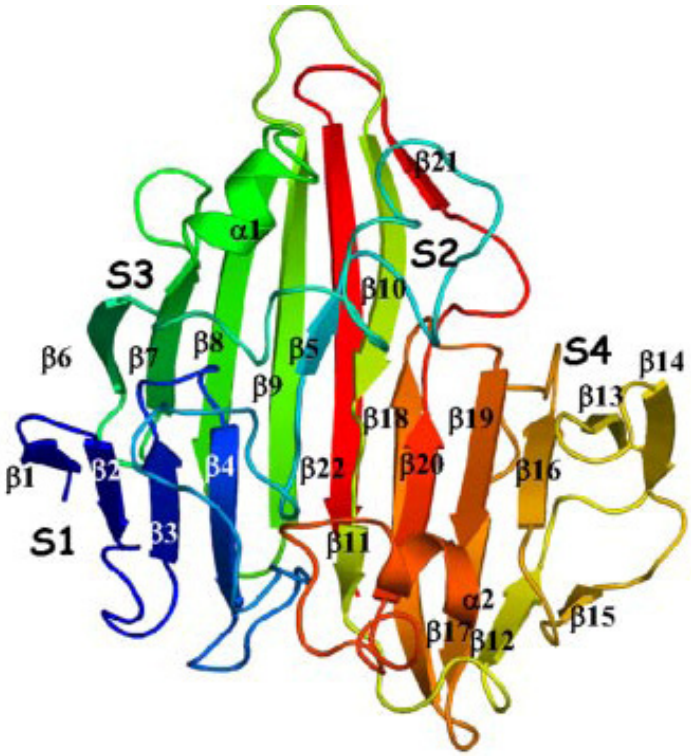

Fig. 8: Stereoview ribbon representation of yeast H6PM (Graille et al. 2006)

A system to knock down the gene by RNAi has been produced in the laboratory of Paul Michels at UCL, Brussels, and by a first study it seems that the enzyme is important for growth of the procyclic trypanosomes (Moebius, thesis).

AIM OF THE STUDY

The objective of this work was to well characterize the enzyme and elucidate its function in *T.brucei* metabolism. Above all the aim has been to assess the importance of the putative H6PM for the insect and mammalian stage of the parasite, for bloodstream form in particular related to oxidative stress defence.

The approach is to use *T. brucei* cell lines (BF and PF) where H6PM is knocked-down by RNAi and to check the effect on the viability of trypanosomes and, for bloodstream form, on their susceptibility to oxidative stress, comparing the results to cell line where G6PDH is depleted and a significant growth reduction was the result, indicating the importance of this pathway.

Furthermore, more generally parasite-specific features of this enzyme should be unravelled, notably to study its inter-relation with the PPP and glycolysis. It might also serve as potential target for new drugs. Compounds may then be developed that will inhibit the enzyme without having an effect on enzymes of the human host. Such inhibitors could serve as leads in the development of new drugs against the diseases caused by the parasites.

MATERIALS AND METHODS

Overexpression of the *T. brucei* enzyme in *E. coli.*

pET28, which has the bacteriophage T7 RNA polymerase promoter, is the expression plasmid while the pJET1/blunt is the cloning vector.

Plasmid pET28 was transformed into *E.coli* strain BL21 (DE3). BL21 (DE3) are *E. coli* cells with the phage DE3 encoding T7 RNA polymerase under the control of the lacUV5 promoter; they represent an optimal system for expression of recombinant proteins in conjunction with pET plasmids. Plasmid directs the synthesis of a construct with an N-terminal 20 residues long extension including six adjacent histidine residues ('His6-tag').

A single transformed colony was grown overnight at 37°C in LB/kan (Luria Bertani broth plus kanamycin). This preculture was then used to inoculate 250 ml of freshly prepared ZYM-5052 Medium (1 % (w/w) Tryptone, 0.5 % (w/v) Yeast Extract,

25 mM Na_2HPO_4, 25 mM KH_2PO_4, 50 mM NH_4Cl , 5 mM Na_2SO_4 , 2 mM $MgSO_4$, 0,5 % Glycerol, 0,05 % Glucose,0,2% Lactose) supplemented with 30 μg/ml kanamycin at 20°C for 17 hours.

Purification of recombinant protein

Cells were harvested by centrifugation (5000 rpm, 20 min), resuspended in 10 mL of cell lysis buffer (50 mM NaH_2PO_4 pH 8, 300 mM NaCl, 10 mM imidazole, 2 mM β-mercaptoetanol) and a complete protease inhibitor cocktail (Roche Applied Science). Cells were disrupted by three passages through a SLM-Aminco French pressure cell (SLM Instruments, Inc.) at 6.9 MPa. Nucleic acids were degraded by incubation of the lysate with 100 units of DNase (Roche Applied Science) for 20 min at 4°C. Cell debris and insoluble material were then spun down (9000 rpm, 10 min).The supernatant was added to a 1,5 ml of Ni-NTA.agarose resin (Quiagen) and was allowed to bind to the resin in a batch format for 1 h at 4°C with gentle agitation. The resin with bound protein was then transferred to a column and washed extensively with wash buffer (20 mM imidazole) and eluted with elution buffer (250 mM imidazole). Samples were analyzed on 10% SDS-PAGE gels.

Determination of protein concentration

Protein content was determined with the spectrophotometer at 280 nm, assuming that a solution containing 1mg/ml of protein have an absorbance of 1 O.D.
Otherwise the Bradford assay for protein quantification was used.

Electrophoresis in polyacrylamide gel (SDS PAGE)

4 µg/µl of enzyme are denatured at 100°C for 5 minutes in the presence of the reducing agent 2-mercaptoethanol and loaded onto a 10 % polyacrylamide gel. The migration has been made into electrophoresis buffer during 45 minute with an amperage of 25 mA. The proteins were coloured with a solution of Comassie blue (0.008% p/v Comassie Brillant Blue G-250, 45 mM HCl) by warming the gel in a microwave oven for about 30-60 sec.
Destaining is done in bidistilled water at room temperature gently shaking.

Storage of the enzyme

Due to its fast inactivation after purification, the enzyme was stored in different conditions to determine the best one to preserve its activity.
The enzyme was stored in the presence of 50% glycerol at -20°C and in 3.2M ammonium sulphate (or more till 80% saturation) at 4°C.

Kinetic studies

Normally it was used for kinetic measurements directly after purification, because of the enzyme instability : a time-dependent decrease of activity was observed after purification.

Preparation of α-glucose

A saturated solution of D-glucose in water is prepared at 45°C and then conserved at 4°C for a long period till crystallisation of α-glucose (Thomson and Wolfrom, 1962).

G6PDH-Assay (Wurster and Hess, 1972, Graille et al., 2006)

In a first assay system to determine the specificity of H6PM for Glc6P (Fig. 9), any formation of β-Glc6P from α-glucose via yeast HK (=HXK) and H6PM could be followed by measuring the increase in absorbance at 340 nm in a Jenway 6715 UV-vis spectrophotometer caused by the generation of NADPH, coupled to the conversion of β-Glc6P into D-glucono-1.5-lactone 6-phosphate by G6PDH. Using instead *T. cruzi* glucokinase in place of exokinase the formation of β-Glc6P from β-glucose could be followed. Measurements were performed at 20°C in 0.1 M triethanolamine (pH 7.6), 2.5 mM $MgCl_2$, 5 mM ATP, 0.64 mM NADP+, 1.4 U of yeast G6PDH, 2 U of HK and 20 mM of either α- or equilibrated glucose.

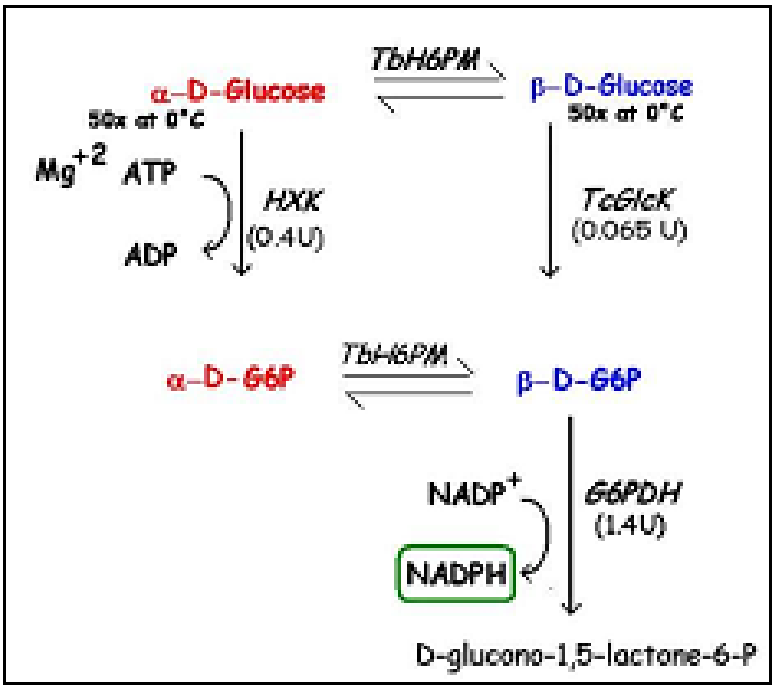

Fig. 9 : Enzymatic assay coupled to G6PDH activity and either HXK or TcGlcK activity or both.

RNA interference

RNA interference is a recently recognized cellular process in which the presence of a double stranded RNA (dsRNA) causes single stranded RNA of the same sequence to be degraded (Ullu et al., 2004). RNAi belongs to a family of related processes referred as post transcriptional gene silencing (PTGS). These pathways were first observed in plants and fungi, since then in trypanosomes, *Drosophila* and other organisms.

The RNAi pathway is initiated by the enzyme Dicer, which cleaves long dsRNA into short fragments of 21-25 nucleotides, termed small interfering RNAs (siRNA). Then only sense strand of each fragment in incorporated into the RNA-induced silencing complex (RISC) that recognizes complementary mRNA molecules and degrades them, resulting in substantially decreased levels of protein translation and effectively turning off the gene (Fig. 10).

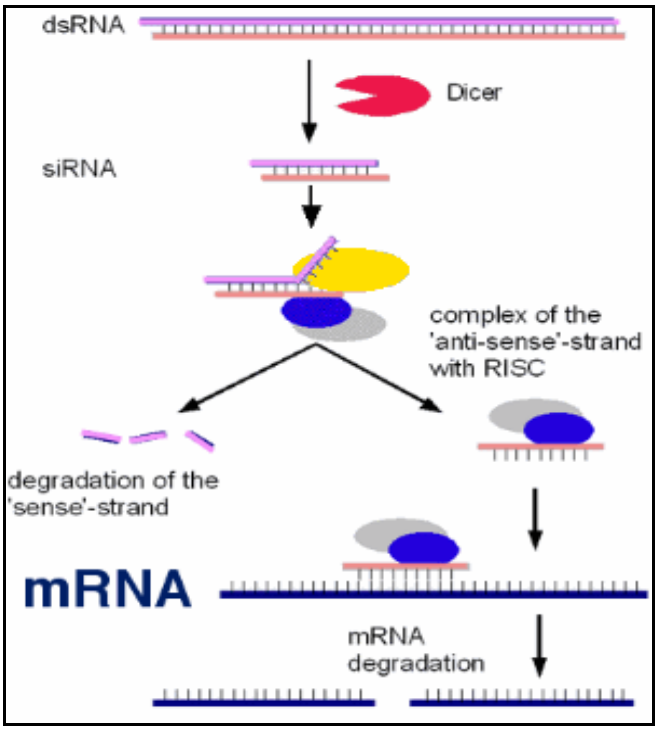

Fig. 10 : Schematic representation of the RNAi pathway in *T. brucei*

RNAi construct

A *T. brucei* specific vector phD677 was used to generate stable bloodstream and procyclic cell lines for the Tetracylin-inducible expression of a double-stranded RNA of putative H6PM. Transgenic trypanosomes (427-strain) that constitutively express the Tet repressor were used for transfection. A DNA fragment containing the full-length gene flanked with HindIII and BamHI restriction sites at the 5'- and 3'- ends, respectively, was introduced into vector pHD677 (Biebinger et al., 1997). This places the gene under the control of a *T. brucei* procyclic acidic repetitive protein promoter (PARP) to which the tet operator has been fused. The vector has also a hygromycin gene, which will be constitutively expressed in trypanosomes, allowing the selection of positive clones (Fig. 11). The recombinant construct is introduced into non-transcribed spacers of the ribosomal RNA repeat.

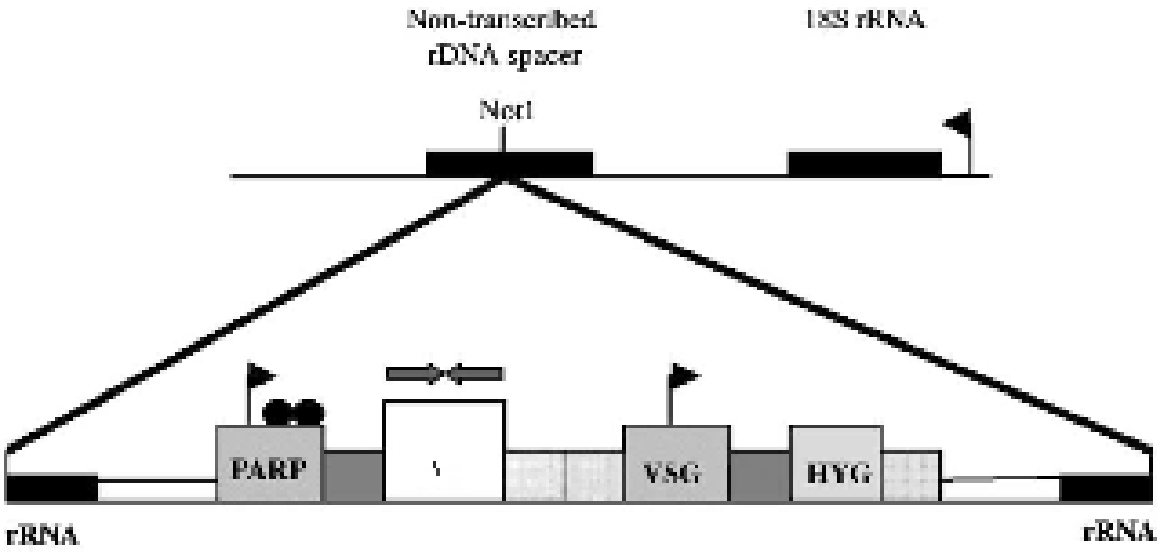

Fig. 11: pDH677 vector. rRNA, intergenic region targeting sequence; the two black circles represent the tetracycline repressor bound to the Tet operator; VSG, constitutive VSG promoter; HYG, hygromicine resistance gene

Double stranded RNAs are produced as hairpin molecules (Fig. 12) by transcription of constructs comprising two complementary fragments of the coding regions of each gene linked by an 50 bp spacer and arranged as a direct inverted repeat.These constructs were obtained by amplification of a sense and an antisense fragment of H6PM using designed primers. The RNAi constructs were

prepared for chromosomal integration in the transcriptionally silent ribosomal RNA gene repeat spacer.

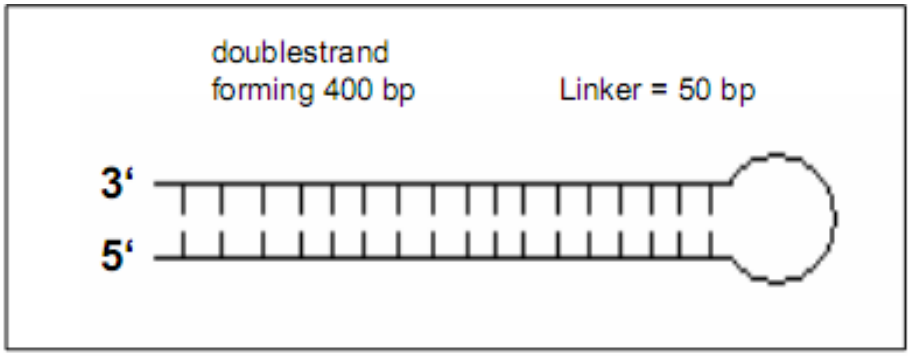

Fig. 12: hairpin formation of double stranded RNA after transcription

Linearization of plasmid

Linearization should be carried out by one hour digestion with 1µl Not1 (1 U/µl) and controlled by agarose gel electrophoresis. Transfection was carried out in triplicate using 10 µg of DNA each time, therefore quantification should be performed after the purification step to assure a total amount of at least 30 µg of DNA.

Spectrophotometric determination of DNA concentration

The DNA concentration was assayed both at 260 nm and 280 nm:

DNA Concentration (µg/ml) = A_{280nm} x 50 µg/ml

The ratio OD_{260}/OD_{280} must be ≥ 1.7 for pure preparation of DNA, if the ratio is < 1.7 it means that in the sample there is protein contamination.

Electrophoresis in agarose gel

The agarose gel was prepared in buffer TAE (0,04 M Tris, 1mM EDTA, 5 mM sodium acetate, taken to pH 7.5 with glacial CH_3COOH) adding ethidium bromide 0,4 μg/ml. Before loading, 0.2 volumes of the following buffer: 0.25 % (p/v) bromine phenol dye, 100 mM EDTA, 50% (v/v) glycerol is added to the sample. After the electrophoretic run, DNA is seen by UVtransillumination, for the fluorescence effect of the ethidium bromide that binds to double stranded DNA.

Transfection of trypanosomes and growth curve

T. brucei bloodstream and procyclic trypanosomes were defrozen, diluted into medium and maintained for one week to obtain a stable and well reproducing colture for transfection.
Bloodstream form and procyclic form were grown in HMI-9 medium (Hirumi et al., 1989) at 37°C and in SDM-79 at 28°C, respectively.
The following transfection procedure is different for procyclic and bloodstream form of *T. brucei* and it will therefore be described apart.

Bloodstream form transfection

For transfection of bloodstream form trypanosomes, 15 ml of culture was harvested at a density of 2 x 10^6 cells/ml, centrifuged at 2000 rpm. The pellet was washed once with 5 ml of Cytomix transfection buffer and resuspended in 1,2 ml of the same solution. The cells were then split and 400μl (approximately 1 x 10^7cells/ml) were mixed each with 10 μg of DNA in a transfection cuvette and subsequently subjected to a single discharge by a Genetronics BTX FCM630 electroporator with a 1.23 kV, 25 Ohm and 50 μF setting, to obtain a pulse with a time constant of about 260 μs. The cells were then rapidly diluted in 12 ml culture medium, supplemented with 20% FCS, and incubated overnight. After 24 hours the culture was diluted once by adding a concentration of 5μg/μl of hygromycine and split into 24 wells plate. Antibiotic-resistant cells were detectable about 5 days after.

Procyclic transfection

For procyclic transfection 6 ml of a culture at 1 x 10^7 cells/ml were centrifuged 10 min at 2000 rpm, washed once with 3 ml ice-cold ZPMF Medium, and resuspended in this medium. 2 x 10^7 cells were mixed each with 10 μg of linearized DNA and incubated on ice in a 4mm electroporation cuvette for 10 min. Cells were then subjected to a single pulse by the electroporator set for a peak discharge of 1.8 kV, 25 Ohm and 50 μF, to give pulse with a time constant of 600-700 μs. After electroporation cells were rapidly diluted in 4.5 ml of SM-79 medium and incubated overnight. Subsequently the culture was diluted serially into 24 wells plate using 4.5 ml conditioned SDM-79 medium (SDM-79 medium harvested from a procyclic culture at the exponential growth phase of 7-9 x 10 cells/ml after one to two days with a light orange colour; elements of this medium are necessary for transfected procyclic forms to recover and start growing) containing 100μg/ml hygromicine (to obtain final concentration of 50 μg/ml).

Antibiotic-resistant cells were detectable about 7 days after.

Positive clones could be selected after the induced period of time by the colour of the medium. Only trypanosomes that introduced the construct, gained antibiotic resistance and were able to grow in the medium, inducing a colour change in the medium from red (HMI-9) or dark orange (SDM-79) to yellow. Then they could be stored at -80 °C in the appropriate medium containing 12 % glycerol or used for RNAi experiments.

For induction of double-stranded RNA, cells were cultured in medium containing 1 g/ml of Tet (in DMSO) for bloodstream-form and 5 g/ml of Tet for procyclic-form cells.

Tet induction has been repeated each 24 hours after counting and diluting and compared to non-induced RNAi cells and to WT trypanosomes.

Cultured cells were diluted daily to $2•10^5$cells/ml and $1•10^6$ cells/ml for bloodstream- and procyclic-form trypanosomes, respectively.

Cell densities were determined using cell counting grids (Bürker-Türk, with a depth of 0.01 mm) and growth curves were plotted as the product of cell density and total dilution, versus time.

RT-PCR

It was performed only on blood-stream form RNAi cell line and WT, to determine how long after induction the levels of the RNA for H6PM decrease, to start oxidative injure test.

Total RNA was extracted with SV total RNA isolation system kit (Promega) from a 50 ml culture of bloodstream form WT and from the same amount of culture of RNAi cell line before tet induction (Non Induced) and after 12, 24, 36, 48, 72 and 96 hours induction.

Amount and purity of RNA was determined by spectrophotometry at 260 and 280 nm.

RT-PCR was performed using 2µg of RNA with random hexamer primers. After a 5 min incubation at 70 °C, ribonuclease inhibitors and dNTP's were added and reaction led for another 5 min at 25 °C.

Reverse transcriptase (Revert Aid H-first strand c-DNA synthesis kit Fermentas) was then used. A control was made without adding the enzyme (RT) to check absence of DNA contamination; a temperature profile was applied (10 min 25 °C, 60 min 42 °C, 10 min 70 °C).

The produced cDNA was either stored at -20°C or immediately used for PCR.

PCR reaction was carried out using GoTaq DNA Polymerase (5 µu/ µl) with green coloured loading buffer (Promega) and 1µg of cDNA for each PCR. Specific primers for H6PM (Table 1) were used to amplify a fragment of 350 bp and tubulin primers as a positive control. The PCR was cycled as written in Table 2.

Table 1: H6PM PCR primers

RT-PCR_fw	5' CGCGATTTGCTTGGACACG 3'
RT-PCR_rv	5' CAACCGCCTTGGCGGCAGCAC3'

Table 2: PCR protocol

Step	Cycles	Temperature	Time
1	1	95 °C	3 minutes
2	16 for Tubuline 26 for H6PM	95 °C 62°C 72°C	30 seconds 30 seconds 30 seconds
3	1	72°C	10 minutes
4	1	4°C	pause

PCR has been repeated three times.
All samples have been loaded on 2% Agarose gel without ethidium bromide and stained afterwards with SyberGold for half an hour under light protection.
Analysis has been carried out with KODAK Image Station in a semi quantitative way. Sum intensity of DNA for the enzyme and for the control protein were evaluated, background by the number of pixels taken in account were subtracted. The so obtained net intensity value for the protein was divided by that for tubuline and the logarithm was calculated. Three independent repetitions of PCR have been carried out and were analysed individually with KODAK Molecular Imaging Software and a mean value could be calculated.

Hydroperoxide-sensitivity assay

RNAi bloodstream trypanosomes grown for 96 hours in the presence and absence of tetracycline were diluted to $2 \cdot 10^5$cells/ml in HMI-9 with hygromycine. Also a WT population was diluted at the same cells density in HMI-9 medium without antibiotic.
Then 25 μM and 125μM H_2O_2 was directly added to the cultures that were incubated at 37°C and 5% CO_2 .
Cells viability was assessed after 6 and 24 hours by counting living parasites in a Burker chamber under the light microscope. Dead parasites were distinguished by morphological and motility criteria.
As a control the same experiment was performed on a cell line transfected with a tet-inducible construct for glucose 6-posphate dehydrogenase (G6PDH) depletion. In this case the hydroperoxide bolus was added after a 24 hours induction.
In a second group of experiments the procedure was standardized and optimized: bloodstream-form trypanosomes (wild-type cells and trypanosomes induced for RNAi) were grown in regular HMI-9 medium. After different periods of time, cells were collected by centrifugation and resuspended in non-reducing medium (modified DMEM, i.e. no β-mercaptoethanol and cysteine). Then the cell density was determined. H_2O_2 was added at different concentrations and the cell suspensions were incubated for 1.5 h; then the cell density was determined again. The procedure was adapted from Krieger et al., 2000.

RESULTS

Conditional depletion of H6PM levels by RNAi

After transfection and dilution, the cells were left in culture, in a medium supplemented with antibiotic, for 5-7 days. Hygromycin resistance caused by expression of the marker gene on the introduced plasmid was used for selection of positive clones. Antibiotic resistant clones continued growing, while parasites not containing the vector died rapidly. For procyclics, three of the 24 clones were positive and, after morphological analysis by light microscopy, one of them was selected for the further studies. For the bloodstream form, only one of the 24 clones was found positive and it was used for RNAi induction.

Growth curves

The growth of trypanosomes, transfected with a plasmid producing double-stranded RNA to decrease the enzyme levels, was determined for cells cultured in the absence (-TET) or presence (+TET) of the RNAi inducer tetracycline (1mg/ml for bloodstream-form trypanosomes and 5 mg/ml for procyclic cells).

For both, bloodstream-form and procyclic trypanosomes, only a small change in the growth rate could be observed upon RNAi induction, compared to WT parasites. Strangely, induced and non-induced trypanosomes follow the same growth rate (Fig. 13 A and B). Usually, non induced cell lines grow at the same rate as WT. This anomalous behaviour could be due to the presence of some antibiotic tracks in fetal calf serum in the medium, otherwise it might suggest 'leakage' of the RNAi control (which sometimes has been reported).

From growth curve it is not possible to determine exactly when RNA level for the protein starts to decrease significantly.

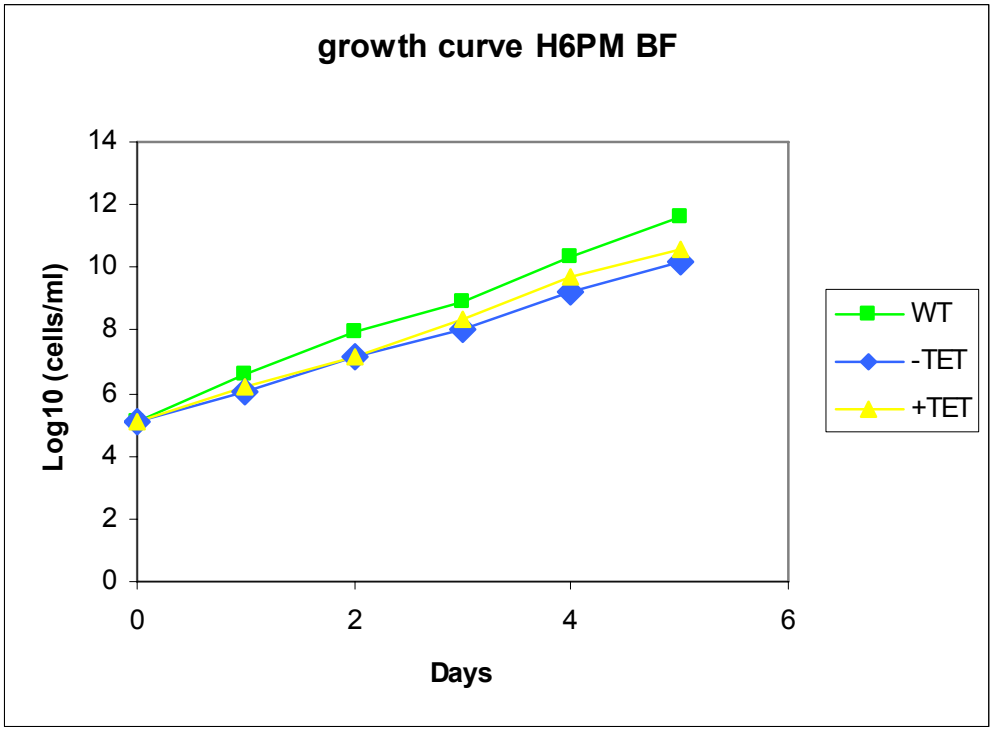

A)

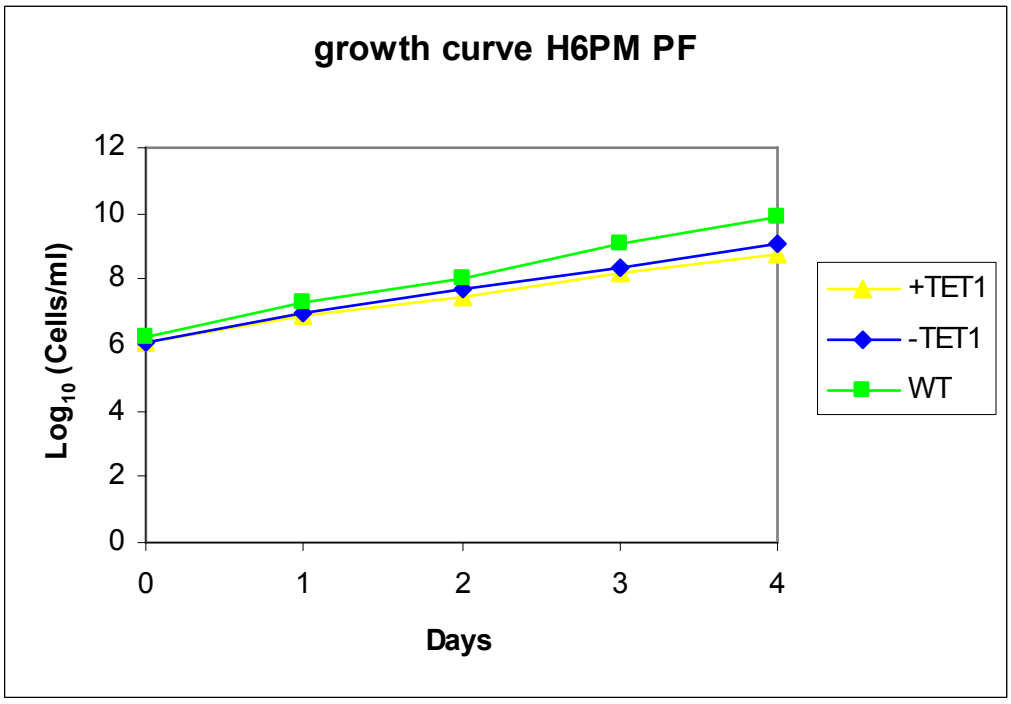

B)

Fig. 13 : Effect of the intracellular depletion of putative tbH6PM by RNAi, on the growth of bloodstream form (A) and procyclic (B) *T. brucei*. In theY axis the $\log_{10}$ values of cumulative cell numbers are shown

RT-PCR

PCR has been carried out (with primers described in Materials and Methods) on cDNA produced from RNA, isolated from bloodstream wild-type trypanosomes, and cells of a cell line, in which the putative tbH6PM was knocked-down by RNA interference, induced by tetracycline.
A control (samples prepared without Reverse Transcriptase) was also subjected to PCR, to assure that false positive amplification results, from co-isolated DNA, are avoided.
24 hours induction sample was not available because of the too low concentration after extraction.

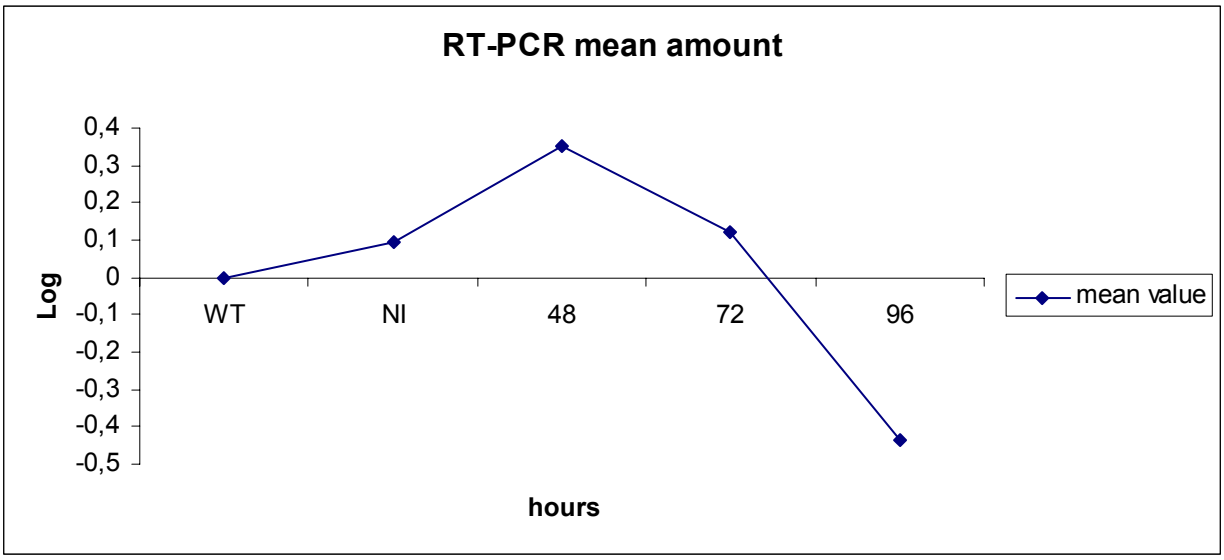

Fig. 14 : RT PCR analysis of bloodstream RNA, over a period of 96 hours induction, with Kodak Molecular Imaging Software and Excel

As shown (Fig. 14 and 15) the RNA level could be reduced by continuous tetracycline induction. The reduction became significant after 72 hours of growth in the presence of inducer and continues until 96 hours. Three independent RT-PCRs have been carried out. The samples were also treated with tubuline primers to get an internal reference. The tubuline RNA amount remains constant during all the time (Fig. 15), so it can be assumed that the same amount of cDNA has been used for RT-PCR. In the control (RNA without reverse transcriptase treatment) a faint band for tubuline

was only detectable in the wild-type cells, so that it can be concluded that no important contamination has taken place during RNA extraction.

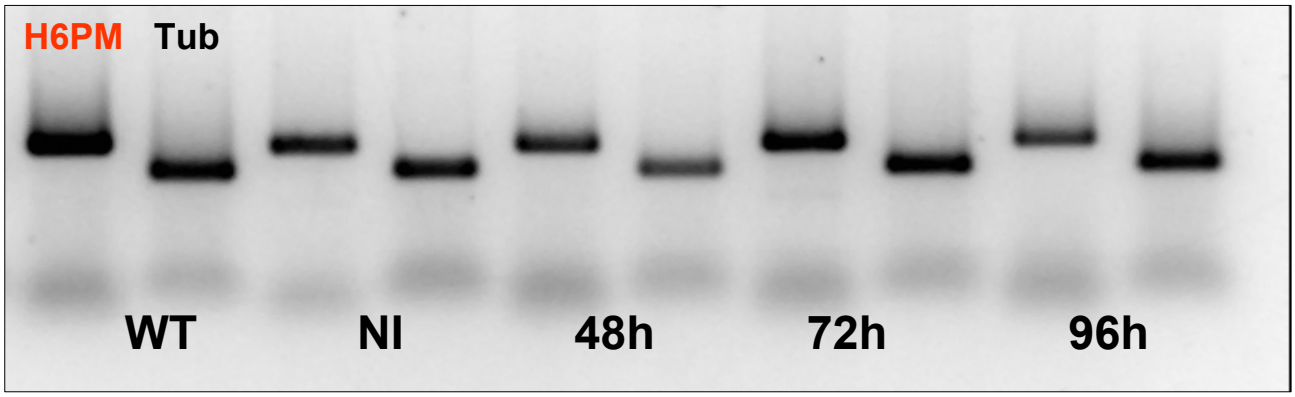

Fig. 15 : Example of RT PCR in agarose gel 1.5%, stained with Sybr gold, imaged with KODAK program (control samples are not shown)

Sensitivity of H6PM-RNAi bloodstream cell lines towards oxidative stress

After 96 hours of induction with tetracycline (as determined from RT-PCR results) trypanosomes depleted of H6PM were diluted to a concentration of $5x10^5$ cells/ml and subjected to oxidative stress produced by addition of a bolus of H_2O_2 at two different concentration: 25 µM and 125 µM. The oxidative stress was induced for 6 and 24 hours, after this period cells viability was assessed by using cell counting grids (Bürker-Türk, with a depth of 0.01 mm) at light microscope.

As a control the same experiment was performed on a cell line transfected with a tet-inducible construct for glucose 6-posphate dehydrogenase (G6PDH) depletion. In this case the hydroperoxide bolus was added after 24 hours induction.

For both cell lines the experiment were repeated twice.

For the latter cell line, it seems (Fig. 16 A and B) that only the highest concentration of H_2O_2 has an effect on the growth rate of parasites and in particular on RNAi cells. Indeed trypanosomes challenged by 25µM H_2O_2 seem not to show a sensitivity increase to oxidative stress.

Otherwise on H6PM RNAi cell line an effect on growth rate was observable also at the lowest concentration of hydroperoxide, but a dramatic effect on the growth rate is visible when the cells are subjected to the highest concentration of H_2O_2 ,this is more evident for the G6PDH RNAi cell line (Fig. 17 A and B and 16 B).

A

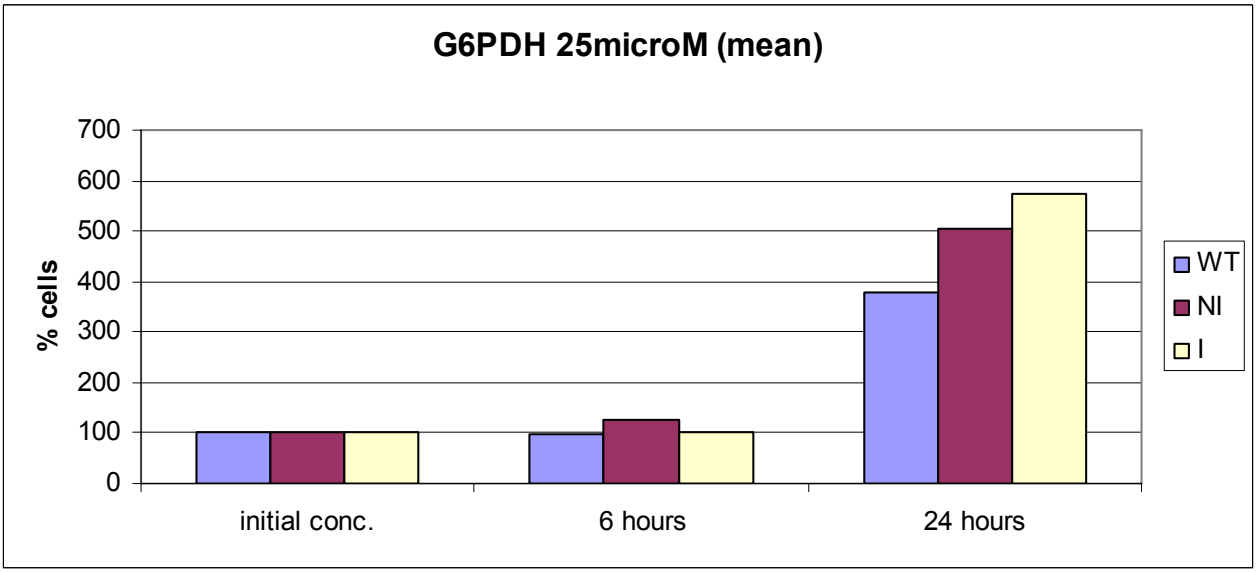

B

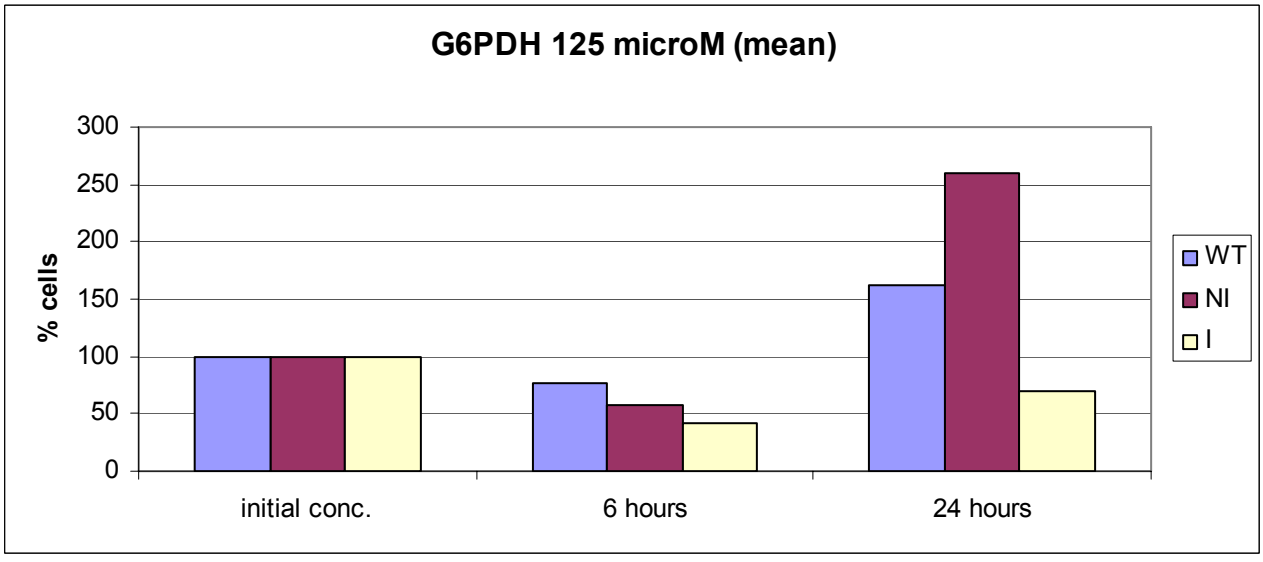

Fig. 16: Susceptibility for H_2O_2 (25 μM and 125 μM) of bloodstream-form trypanosomes in which G6PDH is depleted by RNAi

A

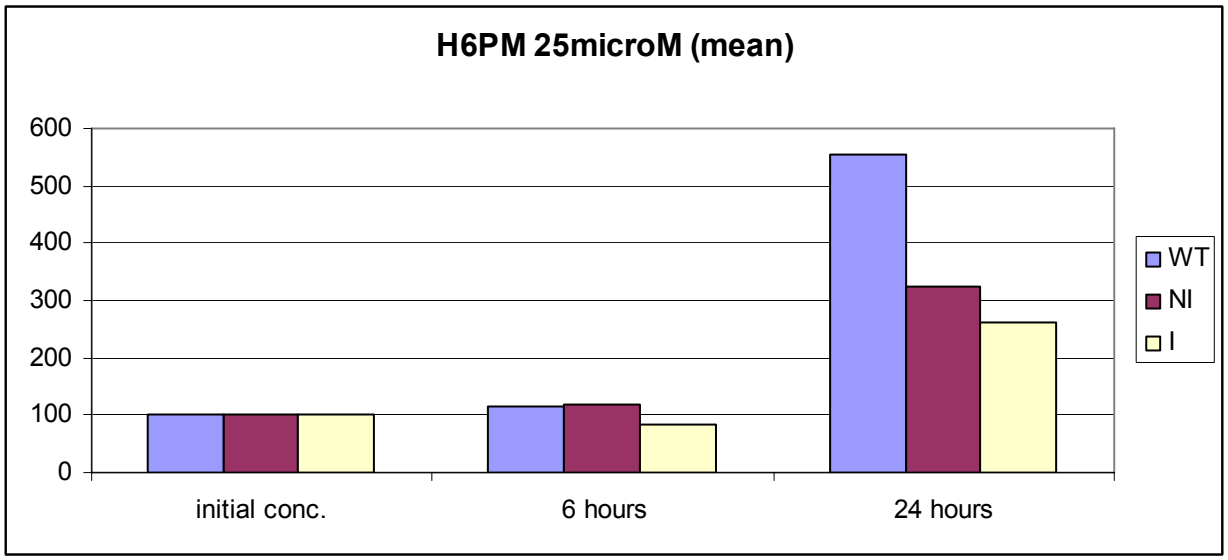

B

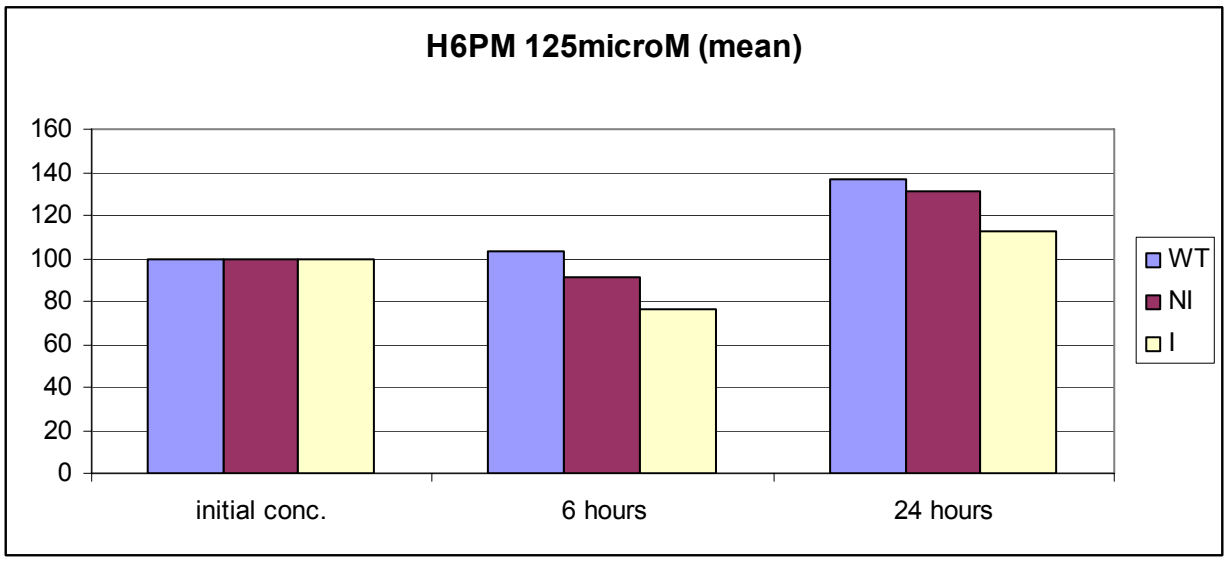

Fig. 17: Susceptibility for H_2O_2 (25 µM and 125 µM) of bloodstream-form trypanosomes in which H6PM is depleted by RNAi

Other experiments where the procedure was optimized using a fresh resuspension modified medium without reducing agents such as β-mercapotoethanol and cysteine, after 24-96 hours of induction of RNAi, showed not only reproducible results but that low oxidant concentration affect cells viability and can kill trypanosomes, almost at at a similar degree of G6PDH RNAi cells (Fig. 18 and 19).

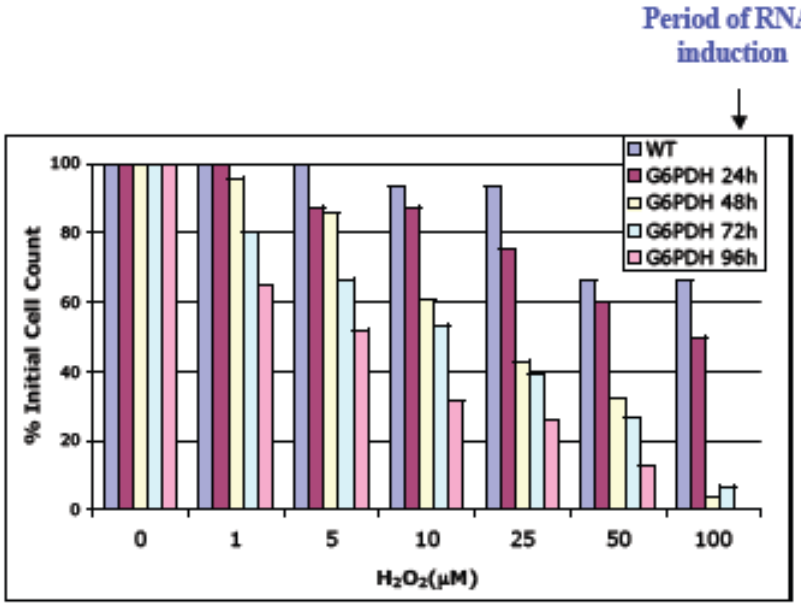

Fig. 18 : Control: The susceptibility for H_2O_2 of bloodstream-form trypanosomes in which glucose-6-phosphate dehydrogenase is depleted by RNAi (results of two independent duplicate experiments)

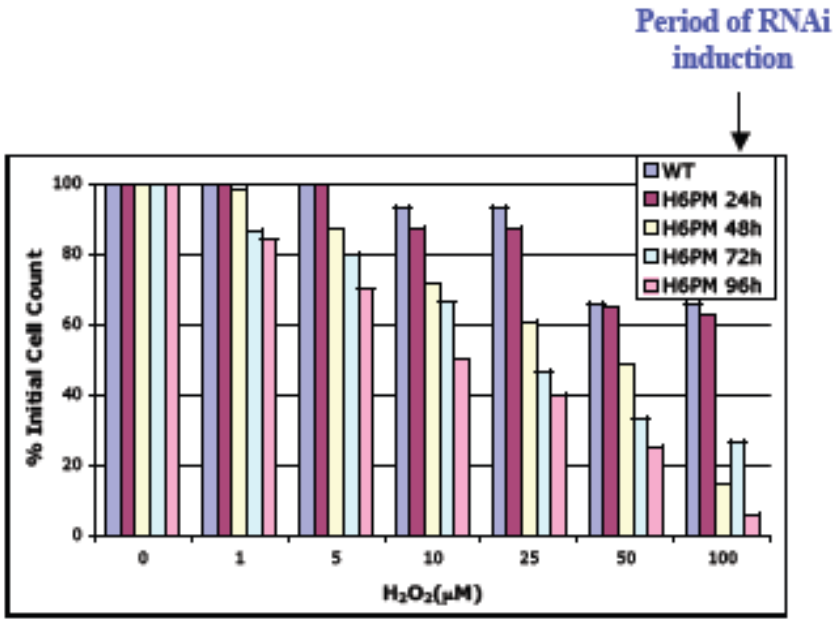

Fig. 19 : The susceptibility for H_2O_2 of bloodstream-form trypanosomes in which the putative exose-6-phosphate-1-mutarotase is depleted by RNAi (results of two independent duplicate experiments)

Protein purification from *E. coli*

During the enzyme preparation, we compared bacteria lysis by sonication and by the use of French press. The last method was necessary to obtain the enzyme. It is reported in fact that much protein remains in inclusion bodies, even if the sequence analysis predicts a good solubility.
In Fig. 18 the purity degree is shown after 250 mM imidazole elution from the Nichel resin specific for proteins with a his tag. Gel filtration is necessary to obtain a definitive pure protein as shown in Fig. 19.

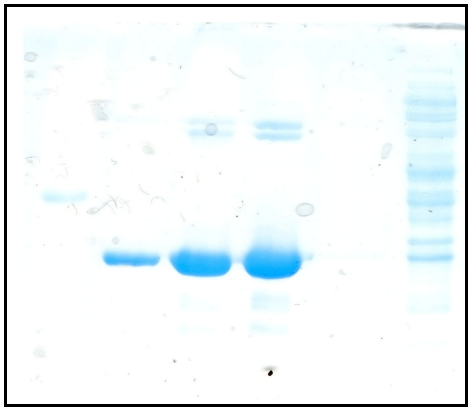

Fig. 18 SDS-PAGE of *T. brucei* H6PM purified from *E. coli*.
In the 2nd lane from the left the most pure fraction eluted by 250 mM imidazole from Ni-NTA resin.
In the 1st lane ovalbumine (45 kDa), in the last lane the not-absorbed sample while in the 3rd and 4th lanes the initial eluted fractions, showing a lower purity degree.

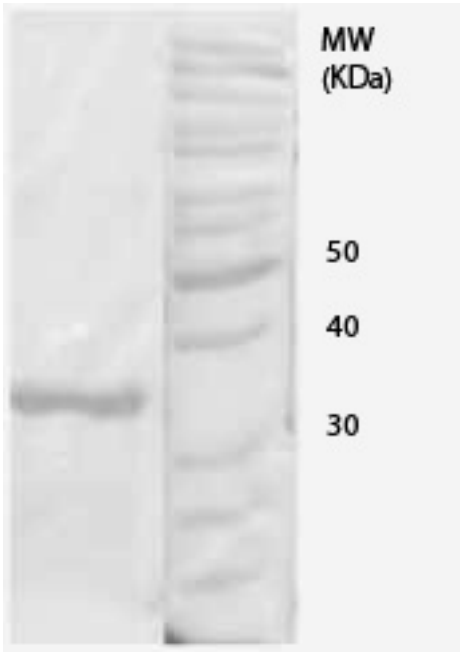

Fig. 19 SDS-PAGE of *T. brucei* H6PM purified from *E. coli*.
In the1st lane from the left pure protein is shown after gel-filtration on a Superdex 200 10/300 column, equilibrated with 50 mM phosphate buffer with 0.15 M NaCl pH 7.0.

Activity assays

To assay H6PM activity first we used as substrate glucose, which is supposed to be a mixture of α and β anomers with a higher β concentration, and, as coupled enzymes, a kinase and G6PDH from yeast which is specific for β−glucose 6P .
When we used H6PM, in association with *T. cruzi* glucokinase which is specific for β−glucose (Scheme 2), we observed a very slight, not very significant, increase of activity, compared to the basal activity without mutarotase.

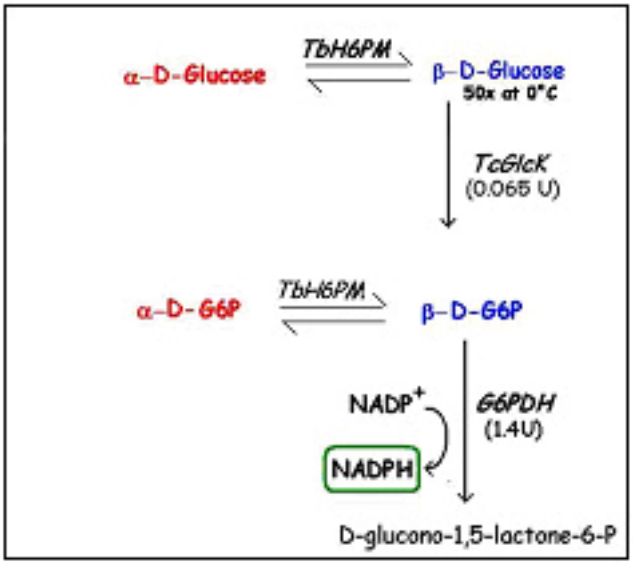

Scheme 2

Instead, using H6PM, in association with yeast exokinase (Scheme 3), which has a preference for α-glucose, we could observe a clear doubling of activity.

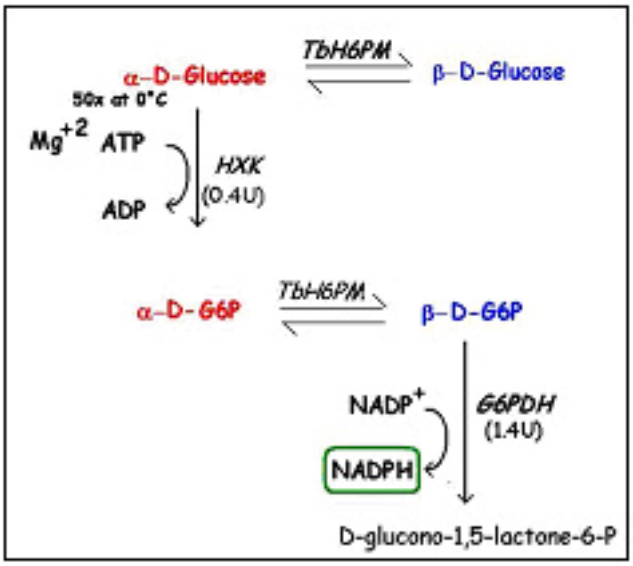

Scheme 3

Same results were obtained using crystallysed α-glucose as starting substrate.

Stability of recombinant *T. brucei* H6PM

Activity decay is very rapid, thus the assay was possible only the same day of purification. Enzyme inactivation was present either by leaving the enzyme at 4°C or in glycerol at -20°C.
Precipitation of H6PM was possible only with a 80% ammonium sulphate saturation but again activity was irreversibly lost after 1 night at at 4°C.

DISCUSSION

Our results suggest that *T. brucei* H6PM is active on glucose-6P as substrate and not on glucose. Same data were obtained using a crystallised α-glucose, suggesting that in solution a very fast equilibrium between the two anomers is present.

Data were previously reported of an activity also on glucose, when tested with an other type of assay, the so called "pyruvate kinase assay", where the substrate is glucose and the coupled enzymes are *T. cruzi* glucokinase, pyruvate kinase and lactic dehydrogenase with addition of ATP, phosphoenolpyruvate, and NADH (Scheme 4)(Moebius thesis).

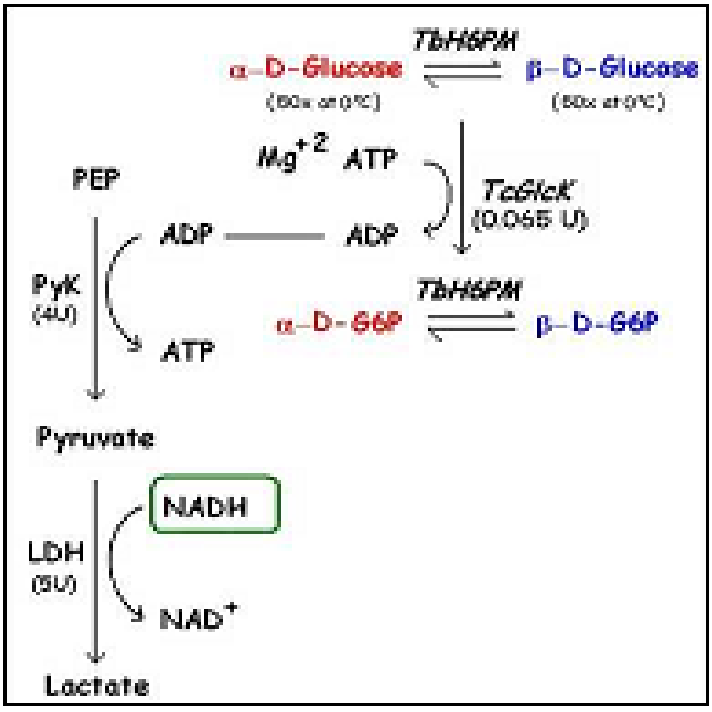

Scheme 4

Anyway *T. brucei* recombinant H6PM is a very unstable enzyme, thus very difficult to assay, even if, using a more pure enzyme, recovered by gel-filtration, might in future studies to improve the stability conditions.

Even if kinetic studies are certainly not exciting, striking results are obtained with RNAi of the studied enzyme in bloodstream trypanosomes. Here the exciting first results are reported, and further optimized studies using a fresh resuspension modified medium without reducing agents such as β-mercapotoethanol and cysteine, after 72-96 hours of induction of RNAi.

Expression knockdown of the putative G6P-1-epimerase by RNAi, has a small effect on growth of bloodstream-form *T. brucei* under normal conditions, but a dramatic effect when the cells are subjected to oxidative stress. H_2O_2 concentrations that have hardly any effect on wild-type cells affect already non-induced cells (suggesting 'leakage' of the RNAi control) and kill the cells upon induction.

Data suggest indeed a role for this putative G6P-1-epimerase, whose better name is hexose-6P mutarotase, in feeding the pentose phosphate pathway (PPP).

So the conclusion is that the H6PM is important for oxidative defence, probably by accelerating the anomeric conversion of G6P so that the flux through the PPP can increase.

Data also confirm that G6PDH and more, PPP, is a good target to hit in African trypanosomes, but the upstream metabolic enzyme H6PM could be hindered too, in search of new approaches to fight these parasites, which often develop resistance to the actual used drugs.

REFERENCES PART I

Amara RR, Robinson HL.” A new generation of HIV vaccines” Trend Molec.Med. 2002 Oct;8(10):489-95

Barillari G, Buonaguro L, Fiorelli V, et al. Effect of cytokines from activated immune cells on vascular cell growth and HIV-1 gene expression. Implications for AIDS–Kaposi’s sarcoma pathogenesis. J Immunol 1992;149:3727–34.

Bayer P, Kraft M, Ejchart A, Westendorp M, Frank R, Rösch P Structural Studies of HIV-1 Tat Protein. *J. MoL Biol* 1995. 247, 529-535

Binley JM,Wrin T, Korber B, et al. 2004. Comprehensive cross-clade neutralization analysis of a panel of anti-human immunodeficiency virus type 1 monoclonal antibodies. J. Virol. 78:13232–52

Cafaro A, Caputo A, Maggiorella MT, et al. SHIV89.6P pathogenicity in cynomolgus monkeys and control of viral replication and disease onset by human immunodeficiency virus type 1 Tat vaccine. J Med Primatol 2000;29:193–208.

Chen B, Vogan EM, Gong H, Skehel JJ, Wiley DC, et alStructure of an unliganded simian immunodeficiency virus gp120 core. Nature 433:834–841. (2005)

Chen L,Kwon YD, ZhouT, et al. 2009. Structural basis of immune evasion at the site ofCD4 attachment on HIV-1 gp120. Science 326(5956): In press

Davis KL, Bibollet-Ruche F, Li H, et al. 2009. Human immunodeficiency virus type 2 (HIV-2)/HIV-1 envelope chimeras detect high titers of broadly reactive HIV-1 V3-specific antibodies in human plasma. J. Virol. 83:1240–59

Ensoli B, Barillari G, Salahuddin SZ, Gallo RC, Wong-Staal F. Tat protein of HIV-1 stimulates growth of cells derived from Kaposi’s sarcoma lesions of AIDS patients. Nature 1990;345:84–7.

Ensoli B, Buonaguro L, Barillari G, et al. Release, uptake, and effects of extracellular human immunodeficiency virus type 1 Tat protein on cell growth and viral trans activation. J Virol 1993;67:277–87.

Ensoli B, Cafaro A. Novel strategies toward the development of an effective vaccine to prevent human immunodeficiency virus infection or acquired immunodeficiency virus. AIDS Clin Rev 2000;01:23–61.

Fanales-Belasio E, Moretti S, Nappi F, et al. Native HIV-1 Tat protein targets monocyte-derived dendritic cells and enhances their maturation, function and antigen-specific T-cell response. J Immunol 2002;168:197–206.

Fouts TR, Binley JM, Trkola A, et al. 1997. Neutralization of the human immunodeficiency virus type 1 primary isolate JR-FL by human monoclonal antibodies correlates with antibody binding to the oligomeric form of the envelope glycoprotein complex. J. Virol. 71:2779–85

Frankel AD, Young JA HIV-1: fifteen proteins and an RNA.Annu Rev Biochem. 1998;67:1-25. Review.

Frost SD, Wrin T, Smith DM, et al. 2005. Neutralizing antibody responses drive the evolution of human immunodeficiency virus type 1 envelope during recent HIV infection. Proc. Natl. Acad. Sci. USA 102:18514–19

Hahn BH, Shaw GM, De Cock KM, Sharp PM AIDS as a zoonosis: scientific and public health implications. Science. 2000 Jan 28;287(5453):607-14. Review.

Hartley O, Klasse PJ, Sattentau QJ, Moore JP. 2005. V3: HIV's switch-hitter. AIDS Res. Hum. Retrovir. 21:171–89

Hoxie J. Toward an Antibody-Based HIV-1 Vaccine Annu. Rev. Med. 2010. 61:135–52

http://hivmedicine.com/index.htm

http://hiv-web.lanl.gov

http://www.hiv1tat-vaccines.info/index.php

Huang, C. C. et al. Structure of a V3-containing HIV-1 gp120 core. Science 310, 1025–1028 (2005

Kim DT, Mitchell DJ, Brockstedt DG, Rothbard JB. Introduction of soluble proteins into the MHC class I pathway by conjugation to an HIV Tat peptide. J Immunol 1997;159:1666–8.

KimM,Qiao ZS,Montefiori DC, et al. 2005. Comparison ofHIV Type 1 ADA gp120 monomers versus gp140 trimers as immunogens for the induction of neutralizing antibodies. AIDS Res. Hum. Retrovir.21:58–67

Klein JS, Gnanapragasam PN, Galimidi RP, et al. 2009. Examination of the contributions of size and avidity to the neutralization mechanisms of the anti-HIV antibodies b12 and 4E10. Proc. Natl. Acad. Sci.USA 106:7385–90

Korber B, Muldoon M, Theiler J, Gao F, Gupta R, Lapedes A, Hahn BH, Wolinsky S, Bhattacharya T Timing the ancestor of the HIV-1 pandemic strains. Science. 2000 Jun 9;288(5472):1789-96
.
Kwong PD, DoyleML, Casper DJ, et al. 2002.HIV-1 evades antibody-mediated neutralization through conformational masking of receptor-binding sites. Nature 420:678–82

Kwong PD, Wyatt R, Robinson J, et al. 1998. Structure of an HIV gp120 envelope glycoprotein in complex with the CD4 receptor and a neutralizing human antibody. Nature 393:648–59

Kwong PD,Wilson IA. 2009.HIV-1 and influenza antibodies: seeing antigens in newways.Nat. Immunol. 10:573–78

Kwong, P.D. et al. Structure of anHIVgp120 envelope glycoprotein in complex with the CD4 receptor and a neutralizing human antibody.Nature 393, 648–659 (1998)

Labrijn AF, Poignard P, Raja A, et al. 2003. Access of antibody molecules to the conserved coreceptor binding site on glycoprotein GP120 is sterically restricted on primary HIV-1. J. Virol. 77:10557–65

Li M, Gao F, Mascola JR, et al. 2005. Human immunodeficiency virus type 1 env clones from acute and early subtype B infections for standardized assessments of vaccine-elicited neutralizing antibodies. J. Virol. 79:10108–25

Liu J, Bartesaghi A, Borgnia MJ, Sapiro G, Subramaniam S. Molecular architecture of native HIV-1 gp120 trimers.Nature;455: 109-13 (2008)

Louie JK, Hsu LC, Osmond DH, Katz MH, Schwarcz SK. "Trends in causes of death among persons with acquired immunodeficiency syndrome in the era of highly active antiretroviral therapy, San Francisco, 1994-1998" J Infect Dis. 2002 Oct 1;186(7):1023-7

Lusso P, Earl PL, Sironi F, et al. 2005. Cryptic nature of a conserved, CD4-inducible V3 loop neutralization epitope in the native envelope glycoprotein oligomer of CCR5-restricted, but not CXCR4-using, primary human immunodeficiency virus type 1 strains. J. Virol. 79:6957–68

Marchio S.` , M. Alfano, L. Primo, D. Gramaglia, L. Butini, L. Gennero, E. De Vivo, W. Arap, M. Giacca, R. Pasqualini, and F. Bussolino Cell surface–associated Tat modulates HIV-1 infection and spreading through a specific interaction with gp120 viral envelope protein Blood. 2005;105:2802-2811

MO, Frank R, Ochsenbauer C, et al. Sensitization of T cells to CD95-mediated apoptosis by HIV-1 Tat and gp 120. Nature 1995;275:497–500.

Moore PL, Crooks ET, Porter L, et al. 2006. Nature of nonfunctional envelope proteins on the surface of human immunodeficiency virus type 1. J. Virol. 80:2515–28

Ott DE, Coren LV, Chertova EN, Gagliardi TD, Schubert U Ubiquitination of HIV-1 and MuLV Gag.VirologyDec 5;278(1):111-21.(2000)

Pierson TC, Doms RW. 2003. HIV-1 entry and its inhibition. Curr. Top. Microbiol. Immunol. 281:1–27

Pitisuttithum P, Gilbert P, Gurwith M, Heyward W, Martin M, van Griensven F, Hu D, Tappero JW, Choopanya K; Bangkok Vaccine Evaluation Group - J Infect Dis. 2006;194(12):1661-71

Preston BD, Dougherty JP.Mechanisms of retroviral mutation.Trends Microbiol. 1996 Jan;4(1):16-21. Review.

Re MC, Furlini G, Vignoli M, et al. Effect of antibody to HIV-1 Tat protein on viral replication in vitro and progression of HIV-1 disease in vivo. J Acquired Immune Defic Syndr Hum Retrovirol 1995; 10:408–16.

Re MC, Vignoli M, Furbini G, et al. Antibodies against full-length Tat protein and some low-molecular-weight Tat-peptides correlate with low or undetectable viral load in HIV-1 seropositive patients. J Clin Virol 2001;21:81–9.

Reiss P, Lange JM, de Ronde A, et al. Speed of progression to AIDS and degree of antibody response to accessory gene products of HIV-1. J Med Virol 1990;30:163–8.
Roux KH, Taylor KA. 2007. AIDS virus envelope spike structure. Curr. Opin. Struct. Biol. 17:244–52

Sattentau QJ, Moore JP. 1995. Human immunodeficiency virus type 1 neutralization is determined by epitope exposure on the gp120 oligomer. J. Exp. Med. 182:185–96

Wei X, Liang C, Götte M, Wainberg MA."Negative effect of the M184V mutation in HIV-1 reverse transcriptase on initiation of viral DNA synthesis."Virology. 2003 Jun 20;311(1):202-12.

Wyatt R, Kwong PD, Desjardins E, et al. 1998. The antigenic structure of the HIV gp120 envelope glycoprotein. Nature 393:705–11

Yamasaki, N., Hayashi, K. and Funatsu, M. (1968) Acetylation of lysozyme. Part I. preparation, fractionation and properties of acetylated lysozyme. Agric. Biol. Chem., 32, 55–63.

Yang X, Kurteva S, Ren X, et al. 2005. Stoichiometry of envelope glycoprotein trimers in the entry of human immunodeficiency virus type 1. J. Virol. 79:12132–47

Yang ZN, Mueser TC, Kaufman J, Stahl SJ, Wingfield PT, Hyde CC The crystal structure of the SIV gp41 ectodomain at 1.47 A resolution. J Struct Biol 126(2): 131-144 (1999)

Zagury JF, Sill A, Blattner W, et al. Antibodies to the HIV-1 Tat protein correlated with nonprogression to AIDS. A rationale for the use of Tat toxoid as an HIV-1 vaccine. J Hum Virol 1998;4:282–92.

Zanetti G, Briggs JA, Grünewald K, Sattentau QJ, Fuller SD.Cryo-electron tomographic structure of an immunodeficiency virus envelope complex in situ.PLoS Pathog;790-797;2(8) (2006)

Zhu T, Korber BT, Nahmias AJ, Hooper E, Sharp PM, Ho DD.An African HIV-1 sequence from 1959 and implications for the origin of the epidemic.Nature. 1998 Feb 5;391(6667):594-7

REFERENCES PART II

Albert MA, Haanstra JR, Hannaert V, Van Roy J, Opperdoes FR, Bakker BM, Michels PA (2005) Experimental and in silico analyses of glycolytic flux control in bloodstream form Trypanosoma brucei, J Biol Chem 280: 28306-28315

Barrett, M.P., Gilbert, I.H. Perspectives for new drugs against Trypanosomiasis and Leishmaniasis. Curr. Top. Med. Chem., 2002, 11, 3205-3214

Bakker BM, Westerhoff HV, Opperdoes FR, Michels PA (2000) Metabolic control analysis of glycolysis in trypanosomes as an approach to improve selectivity and effectiveness of drugs. (review), Mol Biochem Parasitol. 106: 1-10

Berriman M, Ghedin E, Hertz-Fowler C, Blandin G, Renauld H, Bartholomeu DC, Lennard NJ, Caler E, Hamlin NE, Haas B (2005) The genome of the African trypanosome Trypanosoma brucei, Science 309: 416-422

Biebinger S, Wirtz LE, Lorenz P, Clayton C (1997) Vectors for inducible expression of toxic gene products in bloodstream and procyclic Trypanosoma brucei, Mol. Biochem. Parasitol. 85: 99-112

Cáceres AJ, Quiñones W, Gualdrón M, Cordeiro A, Avilán L, Michels PA, Concepción JL (2007) Molecular and biochemical characterization of novel glucokinases from Trypanosoma cruzi and Leishmania spp, Mol. Biochem. Parasitol. 156 (2): 235-245

Colasante C, Ellis M, Ruppert T, Voncken F (2006) Comparative proteomics of glycosomes from bloodstream form and procyclic culture form Trypanosoma brucei brucei, Proteomics 6: 3275-3293

Cordeiro AT, Cáceres AJ, Vertommen D, Concepción JL, Michels PAM and Versées W (2007) The Crystal Structure of Trypanosoma cruzi Glucokinase Reveals Features Determining Oligomerization and Anomer Specificity of Hexose-phosphorylating Enzymes, J. Mol. Biol. 372: 1215-1226

Cordeiro AT, Thiemann OH, Michels PA(2009) Inhibition of Trypanosoma brucei glucose-6-phosphate dehydrogenase by human steroids and their effects on the viability of cultured parasites. Bioorg Med Chem. Mar 15;17(6):2483-9

Duffieux F, Van Roy J, Michels PA, Opperdoes FR (2000) Molecular characterization of the first two enzymes of the pentose-phosphate pathway of Trypanosoma brucei: Glucose-6-phosphate dehydrogenase and 6-phosphogluconolactonase, J Biol Chem. 275: 27559-27565

Fairlamb AH, Blackburn P, Ulrich P, Chait BT, Cerami A. 1985 Trypanothione: a novel bis(glutathionyl)spermidine cofactor for glutathione reductase in trypanosomatids. Science;227(4693):1485-7.

Fairlamb AH, Cerami A.(1992) Metabolism and functions of trypanothione in the Kinetoplastida. Annu Rev Microbiol.;46:695-729.

Graille M, Baltaze JP, Leulliot N, Liger D, Quevillon-Cheruel S, van Tilbeurgh H. (2006) Structure-based Functional Annotation: Yeast ymr099c codes for a D-hexose-6-phosphate mutarotase, J Biol Chem. 281: 30175-30185

Guerra-Giraldez C., Quijada L., Clayton C.E. (2002), Compartmentation of enzymes in a microbody, the glycosome, is essential in Trypanosoma brucei, J Cell Sci. 15: 2651-2658
Hannaert V, Bringaud F, Opperdoes FR, Michels PA (2003) Evolution of energy metabolism and its compartmentation in Kinetoplastida (review), Kinetoplastid Biol Dis. 2:11.

Krauth-Siegel RL, Schöneck R 1995 Flavoprotein structure and mechanism. 5. Trypanothione reductase and lipoamide dehydrogenase as targets for a structure-based drug design FASEB J. Sep;9(12):1138-46.

Krieger et al., 'Trypanosomes lacking trypanothione reductase are avirulent and show increased sensitivity to oxidative stress'. Molecular Microbiology 35 (2000) 542-552.

Livingstone G, Franks F, Aspinall L J (1977) The Effects of aqueous Solvent structure on the mutarotation kinetics of glucose, J. Sol. Chem. 6: 203–216

Malaisse WJ (2003) Metabolism of D-glucose anomers in pancreatic islets (review), Int J Mol Med. 12: 911-916

Michels PA, Bringaud F, Herman M, Hannaert V (2006) Metabolic functions of glycosomes in trypanosomatids (review), Biochim Biophys Acta, 1763 (12): 1463-1477

Nwagwu M, Oppersoes FR (1982) Regulation of glycolysis in Trypanosoma brucei: hexokinase and phophofructokinase activity, Acta Trop. 39: 61-72

Opperdoes FR, Borst P (1977) Localization of nine glycolytic enzymes in a microbody-like organelle in Trypanosoma brucei: the glycosome, FEBS Lett. 80: 360-364

Penninckx MJ, Elskens MT. Metabolism and functions of glutathione in micro-organisms 1993
Adv Microb Physiol.;34:239-301.

Salas M, Vinuela E, Sols A (1965) Spontaneous and enzymatically catalyzed anomerization of Glucose 6-phosohate and anomeric specificity of related enzyme,. J. Biol. Chem. 240 (2): 561-586

Schirmer RH, Schöllhammer T, Eisenbrand G, Krauth-Siegel RL. 1987 Oxidative stress as a defense mechanism against parasitic infections.
Free Radic Res Commun.;3(1-5):3-12.

Thompson JD, Higgins DG, Gibson TJ (1994) CLUSTAL W: improving the sensitivity of progressive multiple sequence alignment through sequence weighting, positionspecific gap penalties and weight matrix choice, Nucleic Acids Res. 22: 4673-4680

Thoden, J B., Holden,H.M. (2002). High Resolution X-ray Structure of Galactose Mutarotase from Lactococcus lactis, J. Biol. Chem. 277: 20854-20861

Van Den Abbeele J, Claes Y, Van Bockstaele D, Le Ray D, Coosemans M (1999) Trypanosoma brucei spp. development in the tsetse fly: characterization of the post-mesocyclic stages in the foregut and proboscis, Parasitology 118: 469–478

Verlinde CL, Hannaert V, Blonski C, Willson M, Perie JJ, Fothergill-Gilmore LA, Opperdoes FR, Gelb MH, Hol WG, Michels PA (2001) Glycolysis as a target for the design of new anti-trypanosome drugs (review), Drug Resist Updat. 4: 50-65

Wurster B, Hess B (1972) Glucose-6-phosphate -1-epimerase from baker's yeast: A new enzyme, FEBS Lett. 23: 341–344